

N72-17591

**NASA CONTRACTOR
REPORT**



NASA CR-1966

NASA CR-1966

**CASE FILE
COPY**

**THEORETICAL STUDY OF CORRUGATED PLATES:
SHEAR STIFFNESS OF A TRAPEZOIDALLY
CORRUGATED PLATE WITH DISCRETE
ATTACHMENTS TO A RIGID FLANGE
AT THE ENDS OF THE CORRUGATIONS**

by Chen-liau Hsiao and Charles Libove

Prepared by

SYRACUSE UNIVERSITY

Syracuse, N.Y. 13210

for Langley Research Center

NATIONAL AERONAUTICS AND SPACE ADMINISTRATION • WASHINGTON, D. C. • FEBRUARY 1972

1. Report No. NASA CR-1966		2. Government Accession No.		3. Recipient's Catalog No.	
4. Title and Subtitle THEORETICAL STUDY OF CORRUGATED PLATES: SHEAR STIFFNESS OF A TRAPEZOIDALLY CORRUGATED PLATE WITH DISCRETE ATTACHMENTS TO A RIGID FLANGE AT THE ENDS OF THE CORRUGATIONS				5. Report Date February 1972	
				6. Performing Organization Code	
7. Author(s) Chen-liau Hsiao and Charles Libove				8. Performing Organization Report No. MAE 1833-T3	
9. Performing Organization Name and Address Syracuse University Department of Mechanical & Aerospace Engineering Syracuse, NY 13210				10. Work Unit No. 134-14-05-02	
				11. Contract or Grant No. NGR 33-022-115	
12. Sponsoring Agency Name and Address National Aeronautics and Space Administration Washington, DC 20546				13. Type of Report and Period Covered Contractor Report	
				14. Sponsoring Agency Code	
15. Supplementary Notes					
16. Abstract <p>Analysis and numerical results are presented for the elastic shear stiffness of a corrugated shear web with a certain type of discrete attachments at the ends of the trough lines of the corrugations, namely point attachments to a rigid flange which interferes with the deformations of the end cross sections by preventing downward movement but permitting upward (lifting off) movement.</p> <p>The analysis is based on certain assumed modes of deformation of the cross sections in conjunction with the method of minimum total potential energy and the calculus of variations in order to obtain equations for the manner in which the assumed modes of deformation vary along the length of the corrugation.</p> <p>The numerical results are restricted to the case of equal-width crests and troughs but otherwise apply to a wide variety of geometries. They are in the form of graphs which give the overall shear stiffness as a fraction of the overall shear stiffness that could be obtained by having continuous attachment at the ends of the corrugations.</p>					
17. Key Words (Suggested by Author(s)) Corrugated shear webs Shear stiffness Discrete attachments				18. Distribution Statement Unclassified - Unlimited	
19. Security Classif. (of this report) Unclassified		20. Security Classif. (of this page) Unclassified		21. No. of Pages 70	
				22. Price* \$3.00	

PREFACE

This is the third in a series of reports dealing with the behavior of corrugated plates. The two previous reports in the series are:

"Theoretical Study of Corrugated Plates: Shearing of a Trapezoidally Corrugated Plate with Trough Lines Held Straight," by Chuan-jui Lin and Charles Libove. Syracuse University Research Institute Report MAE 1833-T1, May 1970. (NASA CR-1749)

"Theoretical Study of Corrugated Plates: Shearing of a Trapezoidally Corrugated Plate with Trough Lines Permitted to Curve," by Chuan-jui Lin and Charles Libove. Syracuse University Research Institute Report MAE 1833-T2, June 1970. (NASA CR-1750)

CONTENTS

	Page
PREFACE	iii
LIST OF FIGURES	vi
SUMMARY	1
INTRODUCTION.	2
Acknowledgment	3
SYMBOLS	4
METHOD OF ANALYSIS.	5
Statement of problem	5
Idealization of the rigid flanges.	6
Solution by means of superposition	7
Solution of problems I, II, and III	10
NUMERICAL RESULTS AND DISCUSSION.	11
Geometries considered.	11
Elastic properties assumed	13
Dimensionless stiffness parameter.	13
Typical results.	14
General results.	16
Further reduction in the number of parameters.	16
Comparison of different end attachment conditions.	17
ILLUSTRATIVE APPLICATION	18
CONCLUDING REMARKS	21
APPENDIX I: SOLUTION OF PROBLEM I.	23
APPENDIX II: SOLUTION OF PROBLEM II.	32
APPENDIX III: SOLUTION OF PROBLEM III.	46
REFERENCE	49
FIGURES	50

LIST OF FIGURES

- Figure 1. -- Cross section considered.
- Figure 2. -- Types of end attachments considered in reference 1.
- Figure 3. -- Type of end attachments considered in the present paper.
- Figure 4. -- (a) Front view and (b) top view of unsheared corrugated plate.
(c) Top view of sheared corrugated plate.
- Figure 5. -- (a) Deformation of end cross section ($z=b$) in the case of point attachments only. (b) Deformation of end cross section ($z=b$) in the case of point attachments to a rigid flange. (c) Simplified representation of rigid flange at $z=b$.
- Figure 6. -- Problems to be superimposed in order to represent the shearing of a corrugated plate with point attachments to a rigid flange.
- Figure 7. -- The loading of figure 6(b) decomposed into a symmetrical and an antisymmetrical component.
- Figure 8. -- Shear stiffness for a particular cross-sectional geometry ($f/p = .3$, $h/p = .3$) and three ratios of thickness to pitch.
- Figure 9. -- Data of figure 8 replotted with t/p incorporated in the abscissa.
- Figure 10. -- Summary of all computed data on dimensionless stiffness Ω .
- Figure 11. -- Data of figure 10 replotted with h/p incorporated in the abscissa.
- Figure 12. -- Data of figure 11 replotted with f/p incorporated in the abscissa.
- Figure 13. -- Comparison of shear stiffness for three different end attachment conditions.
- Figure 14. -- Corrugated shear web in hinged picture frame test fixture, used for illustrative example.
- Figure 15. -- Degrees of freedom of cross-sectional deformation assumed in the solution of problem I.
- Figure 16. -- Degrees of freedom of cross-sectional deformation assumed in the solution of problem II.

THEORETICAL STUDY OF CORRUGATED PLATES:
SHEAR STIFFNESS OF A TRAPEZOIDALLY CORRUGATED PLATE WITH
DISCRETE ATTACHMENTS TO A RIGID FLANGE AT THE ENDS
OF THE CORRUGATIONS

By

Chen-liau Hsiao* and Charles Libove**
Syracuse University

SUMMARY

Analysis and numerical results are presented for the elastic shear stiffness of a corrugated shear web with a certain type of discrete attachments at the ends of the trough lines of the corrugations, namely point attachments to a rigid flange which interferes with the deformations of the end cross sections by preventing downward movement but permitting upward (lifting off) movement.

The analysis is based on certain assumed modes of deformation of the cross sections in conjunction with the method of minimum total potential energy and the calculus of variations in order to obtain equations for the manner in which the assumed modes of deformation vary along the length of the corrugation.

The numerical results are restricted to the case of equal-width crests and troughs but otherwise apply to a wide variety of geometries. They are in the form of graphs which give the overall shear stiffness as a fraction of the overall shear stiffness that could be obtained by having continuous attachment at the ends of the corrugations.

*Graduate Assistant

**Professor of Mechanical and Aerospace Engineering

INTRODUCTION

Corrugated plates have been proposed for use as shear webs in high-speed aircraft, because their accordion-like ability to expand and contract can circumvent the high thermal stresses that might otherwise occur due to large temperature differences between the inner and outer structure of the aircraft. In such applications discrete, rather than continuous, attachments may exist between the ends of the corrugations and the neighboring structure (e.g., the spar caps). It thus becomes important to be able to predict the stresses, deformations, and overall shear stiffness of a corrugated shear web with various kinds of discrete attachments at the ends of the corrugations. The present paper continues the work of an earlier paper (ref. 1) in dealing with this problem, taking up a type of discrete end attachment condition not considered therein.

The type of cross section considered in reference 1 and the present paper is the trapezoidal cross section shown in figure 1. The end attachments considered in reference 1 are shown schematically in figure 2. They are: (a) point attachments at the ends of the trough lines, (b) point attachments at the ends of the crest lines and the trough lines, and (c) wide attachments clamping the entire widths of the trough ends to a rigid flange. The point attachments referred to above are idealizations intended to represent the restraint furnished by small attachments, such as spot welds or clips. They are assumed to provide restraint against displacement, but to offer no resistance to rotation.

The present paper considers an end attachment intermediate to those of figures 2(a) and 2(c), in regard to the severity of the interference

it provides to the deformation of the end cross sections in their own planes. It consists of point attachments to a rigid flange at the ends of the trough lines, as shown schematically in figure 3. The rigid flange prevents downward, but not upward, deflection of the ends of the corrugations. The point attachments in the present analysis are intended to represent attachments, such as rivets or spot welds, which are small in comparison with the widths of the troughs in which they lie. Actual small attachments will, of course, have finite, rather than zero, width and will provide some localized restraint against rotation. Both of these factors are neglected in the present analysis.

Linear elasticity, isotropy of the material, and small deformations are assumed throughout. The width of the plate (i.e., the dimension perpendicular to the direction of the corrugations is assumed to be infinite, so that all the corrugations deform in an identical manner, and the analysis may then be based on a single corrugation. Thus the present analysis will be applicable to finite-width plates if the width is sufficiently great for the attachments along the sides to have a negligible effect on the deformations of most of the corrugations. At the present time, it is difficult to state a criterion for judging when this condition is satisfied.

Acknowledgement. - The work reported herein was done under grant NGR 33-022-115 from the National Aeronautics and Space Administration.

SYMBOLS

b	one-half the length of the corrugations (see fig. 4)
e	one-half the width of a trough (see fig. 1)
f	width of a crest (see fig. 1)
F	shear force on cross sections parallel to the corrugation direction (see fig. 4)
F'	same as F, but for the case of continuous attachment at the ends of the corrugations
G	shear modulus
G_{eff}	effective shear modulus of corrugated plate
h	height of corrugation (see fig. 1)
k	width of inclined plate elements (see fig. 1)
K	shear stiffness, $F/2u_0$
K'	shear stiffness for the case of continuous attachment at the ends of the corrugation, $F'/2u_0$
L	length of corrugations, $2b$
m,n	numerical exponents
p	pitch of the corrugation (see fig. 1)
p'	developed width of one corrugation, $2e + f + 2k$
t	sheet thickness (see fig. 1)
u_0	one-half the relative longitudinal displacement of two adjacent trough lines (see fig. 4)
z	coordinate (see fig. 4)
γ	overall shear strain, $2u_0/p$ (see fig. 4)
θ	angle of sloping plate elements with respect to horizontal (see fig. 1)
Ω	dimensionless stiffness parameter, K/K'

METHOD OF ANALYSIS

Statement of problem. - Figures 4(a) and 4(b) show an end view and a top view, respectively, of the unsheared corrugated plate, and 4(c) shows a top view of the sheared plate. The shearing is accomplished by rotating the flanges through the small angle γ so as to produce a relative longitudinal sliding of the imaginary lines such as mn and pq connecting the frontward ($z=b$) and rearward ($z=-b$) attachment points. The relative advance of any one such line with respect to its rightward neighbor will be denoted by $2u_o$. This relative sliding and the apparent or overall shear strain γ are related by

$$\gamma = \frac{2u_o}{p} \quad (1)$$

It should be noted that the material lines such as mn and pq of figure 4(b) do not remain straight during the shearing of the plate. They, along with the other generators, can be expected to curve, as shown in figure 4(c).

A complete description of the problem requires a statement as to whether or not the flanges are permitted to move relative to each other in the z -direction during the shearing of the plate -- i.e., whether or not the distance between points such as m and n is allowed to change when the plate is sheared. There are two limiting assumptions that can be made in this regard: Either the flanges are not permitted any relative z -wise movement, in which case external forces may be required to prevent such movement, which forces would put the corrugation cross sections (perpendicular to the z -axis) into tension or compression;

or the flanges are permitted freely to separate or come together, in which case there is no resultant tension or compression on the cross section of any corrugation. The latter condition will be assumed in the present paper, because it is felt to be more representative of the state of affairs in an aircraft wing, in which the flanges are essentially the top and bottom spar caps, whose relative movement toward or away from each other is only feebly prevented by the ribs and their own bending stiffnesses.

All longitudinal cross sections will carry the same shear force F , shown in figure 4(c), which can be expected to be proportional to u_0 . Thus

$$F = Ku_0 \quad (2)$$

and the proportionality constant K is a measure of the overall shear stiffness of the corrugated plate. The objective of the present analysis is to determine K or any equivalent stiffness measure. The following sections explain how this objective is accomplished.

Idealization of the rigid flanges. - Figure 5(a) shows, by means of the dotted lines, the deformation of the end cross section ($z=b$) of a corrugated plate sheared as in figure 4(c), with point attachments at the ends of the trough lines, but without the rigid flanges. This problem was solved in reference 1. It is seen that the corners labeled A deflect downward, while the other corners of the troughs deflect upward. (At the opposite end ($z=-b$) the corner deflections are the reverse of those at $z=b$; this may be seen by referring to fig. 6(a).) The effect of the rigid flange is to prevent any downward deflection. Thus the cross-sectional deformation at $z=b$ for the case of interest here

may look as shown in figure 5(b). For the sake of simplifying the analysis, the constraint furnished by the rigid flange will be replaced by the nearly equivalent constraint shown in figure 5(c). That is, the constraint against downward deflection is assumed to be localized at certain corners (those which would deflect downward if the flange were not there), rather than distributed across the entire width of each trough. This represents a slight relaxation of the actual constraint, leading perhaps to a slight under-estimate of the overall shear stiffness.

Solution by means of superposition. - Summarizing the above discussion, the problem as it now stands is to analyze a corrugated plate sheared as shown in figure 4(c), having point attachments at the ends of the trough lines, localized constraints against downward deflection at the corners labeled A in end cross section $z=b$, and similar localized constraints against downward deflection at the adjacent corners in the cross section at the other end, $z=-b$.

The solution of this problem can be obtained by superimposing the solutions of two other problems, which are shown in figures 6(a) and (b). In the first of these problems (fig. 6(a)) the localized constraints are removed and the plate is sheared as in figure 4(c). This is the problem solved in reference 1. During the shearing, the corners labeled A will deflect downward an amount proportional to u_0 , these deflections are therefore labeled $\alpha_1 u_0$ in figure 6(a). The shear force F_1 required to shear the plate will also be proportional to u_0 , and it is therefore denoted by $K_1 u_0$ in figure 6(a). Both the influence coefficient α_1 and the stiffness K_1 are, in principle, obtainable from the solution of this problem in reference 1.

In the second problem (fig. 6(b)), which has not previously been

solved, the plate is loaded with concentrated upward forces of magnitude $2P$ at the corners labeled A, while lines such as mn and pq are prevented from shifting longitudinally with respect to each other (i.e., any overall shear strain is suppressed) but not prevented from lengthening or shortening.* Under this loading there will be upward deflections of magnitude C_2P at the loaded corners and shearing forces of magnitude $F_2 = \alpha_2P$ on all longitudinal cross sections, the latter representing whatever shear force may be necessary to prevent overall shear deformation under this loading. The determination of the compliance C_2 and influence coefficient α_2 requires an analysis of the problem represented by figure 6(b).

By superimposing figures 6(a) and 6(b), one obtains the original problem of a plate with an imposed overall shear strain of $2u_0$ per corrugation and concentrated reactions of magnitude $2P$ due to the presence of the rigid flanges, idealized as in figure 5(c). The magnitude of P is defined by the requirement of zero vertical deflection at the corners labeled A; that is $\alpha_1u_0 - C_2P = 0$, whence

$$P = \alpha_1u_0/C_2 \quad (3)$$

The shear force F is obtained by adding the shear forces F_1 and F_2 of the two substitute problems (figs. 6(a) and (b)). Thus

$$\begin{aligned} F &= F_1 + F_2 \\ &= K_1u_0 + \alpha_2P \\ &= K_1u_0 + \frac{\alpha_2\alpha_1u_0}{C_2} \\ &= (K_1 + \frac{\alpha_2\alpha_1}{C_2}) u_0 \end{aligned} \quad (4)$$

*See second paragraph under "Statement of problem."

Comparing equations (4) and (2), it is evident that the stiffness K which is being sought is given by the formula

$$K = K_1 + \frac{\alpha_2 \alpha_1}{C_2} \quad (5)$$

where K_1 , α_1 , α_2 , C_2 are quantities obtained by solving the two subsidiary problems shown in figure 6.

In order to facilitate the solution of the problem shown in figure 6(b), the loading in that problem will first be decomposed into the two components shown in figures 7(a) and 7(b). Each of these component loadings possesses a symmetry or antisymmetry which will produce a corresponding symmetry or antisymmetry of the deformations. The superposition of the two loadings gives the loading of figure 6(b). Thus the solution of the problem of figure 6(b) can be replaced by the solution of the two simpler problems of figure 7. These will now be discussed in more detail.

Under the completely symmetrical loading of figure 7(a) there will be no tendency for an overall shear deformation to develop, and therefore there will be no resultant shear force required on any longitudinal section to suppress this deformation. The corners labeled A will deflect upward an amount proportional to P. Their deflection can therefore be denoted C_3P .

Under the antisymmetrical loading of figure 7(b) a shear force will be required on longitudinal sections in order to prevent the overall shear deformation which would otherwise occur. Since there is no resultant longitudinal shear force due to the symmetrical loading component (fig. 7(a)), the shear force due to the antisymmetrical component must be the same as that shown in figure 6(b). It is therefore labeled $F_2 = \alpha_2 P$

in figure 7(b). This loading component will also produce an upward deflection of the corners labeled A, of an amount proportional to P and therefore denoted C_4P in figure 7(b).

The sum of the deflections C_3P and C_4P of figure 7 must equal the deflection C_2P of figure 6(b). Therefore

$$C_2 = C_3 + C_4 \quad (6)$$

and equation (7) becomes

$$K = K_1 + \frac{\alpha_2 \alpha_1}{C_3 + C_4} \quad (7)$$

Thus the determination of the shear stiffness K for the original problem (fig. 4) depends upon the solution of three subsidiary problems represented by figures 6(a), 7(a), and 7(b). These will be called problems I, II, and III, respectively. From their solutions certain stiffness, compliance, and influence coefficients are to be abstracted for use in the right-hand side of equation (7): Problem I will yield α_1 and K_1 ; problem II, C_3 ; and problem III, α_2 and C_4 .

Solution of problems I, II, and III. - The solutions of problems I, II and III are described in some detail in appendixes I, II and III, respectively. Here let it suffice to say that each solution is an approximate one based on the method of minimum potential energy. Only a single corrugation needs to be considered, and for each cross section certain degrees of freedom are allowed for the deformation of the cross section in its own plane and normal to its own plane. Thus, the deformation of the corrugation is described in terms of a finite number of cross-sectional deformation parameters, each being a function of the cross-section location — i.e., a function of z . The total potential energy of the corrugation is

written as a functional of these deformations parameters. By means of the calculus of variations, linear differential equations and boundary conditions are obtained, defining as functions of z those cross-sectional deformation parameters which minimize the total potential energy. These differential equations are solved by standard means, and from the solutions the constants required in equation (7) are evaluated.

NUMERICAL RESULTS AND DISCUSSION

Geometries considered. - By the method described above, numerical data on overall shear stiffness were obtained for a variety of geometries, all restricted, however, to the case of equal width crests and troughs (i.e., $f=2e$). With equal width crests and troughs, the cross-sectional shape is defined to within a scale factor by the ratios f/p , h/p , and t/p . The following numerical values were taken for these ratios:



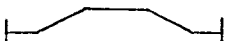
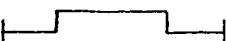


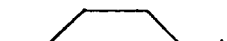


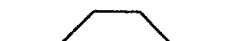
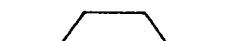
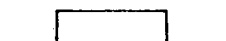

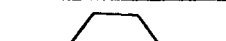
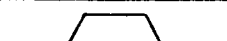
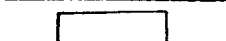

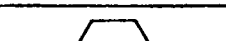
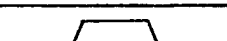
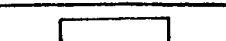
$$f/p = .1, .2, .3, .5$$

$$h/p = .1, .2, .3, .4, .5$$

$$t/p = .005, .015, .025$$

giving $4 \times 5 \times 3 = 60$ different cross sections. With f/p ($=2e/p$), h/p , and t/p fixed, the remaining geometrical properties of the cross section are automatically determined. Table 1 gives, for each f/p and h/p combination, the values of some of these other properties. The first numerical entry in each box is the angle θ in degrees, the second the ratio k/p , and the third the ratio p'/p , where $p' = 2e + f + 2k$ is the developed width of a corrugation. Also shown in each box of the table is a sketch of the cross section.

Table 1. Geometrical properties of cross section considered in calculations

f/p h/p	.1	.2	.3	.5
.1	 $\theta = 14.04^\circ$ $k/p = 0.41$ $p'/p = 1.02$	 18.43° 0.32 1.03	 26.67° 0.22 1.05	 90.00° 0.10 1.20
.2	 $\theta = 26.57^\circ$ $k/p = 0.45$ $p'/p = 1.09$	 33.69° 0.36 1.12	 45.00° 0.28 1.17	 90.00° 0.20 1.40
.3	 $\theta = 36.87^\circ$ $k/p = 0.50$ $p'/p = 1.20$	 45.00° 0.42 1.25	 56.31° 0.36 1.32	 90.00° 0.30 1.60
.4	 $\theta = 45.00^\circ$ $k/p = 0.57$ $p'/p = 1.33$	 53.13° 0.50 1.40	 63.43° 0.45 1.49	 90.00° 0.40 1.80
.5	 $\theta = 51.34^\circ$ $k/p = 0.64$ $p'/p = 1.48$	 59.04° 0.58 1.57	 68.20° 0.54 1.68	 90.00° 0.50 2.00

For each cross-sectional geometry, values of the length parameter $2b/p$ were selected, ranging from 0.4 to 2000. This range is felt to be sufficiently large to cover all cases of practical interest.

Elastic properties assumed. - For the calculations an isotropic material was assumed, with Poisson's ratio ν taken as 0.3, giving .385 as the corresponding ratio of shear modulus G to Young's modulus E .

Dimensionless stiffness parameter. - In presenting the results it will be more efficient to employ a dimensionless stiffness parameter Ω , rather than the dimensional parameter K discussed earlier. The dimensionless stiffness parameter is defined as follows:

$$\Omega = K/K' \quad (8)$$

where K' is the value of K for an identical corrugated plate with continuous attachment at the ends of the corrugations of such a nature as to produce a uniform shear strain throughout the plate.*

The stiffness K' , which is an upper limit to the stiffness achievable with discrete attachments, can be readily computed as follows: In a uniform shear deformation in which line mn in figure 4 advances an amount $2u_0$ with respect to line pq , the uniform shear strain in the plate material must be $2u_0/p'$, where

$$p' = 2e + f + 2k \quad (9)$$

is the developed width of one corrugation. The shear force F' required to maintain this deformation is

$$F' = G \cdot t \cdot 2b \cdot \frac{2u_0}{p'} \quad (10)$$

where G is the shear modulus of the material. Therefore

$$K' \equiv F'/u_0 = \frac{4Gtb}{p'} \quad (11)$$

*Such a condition of uniform shear strain could, in principle, be achieved by having the end cross sections welded to a thin diaphragm which is infinitely stiff with respect to deformations in its own plane but offers no resistance to deformations normal to its own plane (warping deformations of the cross section).

It is a simple matter to convert the dimensionless Ω into the dimensional K (via the relationship $K = \Omega K'$) or into any other stiffness parameter which may be preferred. One such other stiffness parameter might be the ratio of the shear stress $F/2bt$ to the overall shear strain γ shown in figure 4. This ratio, which is essentially an effective shear modulus, is given by

$$\begin{aligned}
 G_{\text{eff}} &= \frac{F/2bt}{\gamma} = \frac{Ku_o/2bt}{\frac{2u_o}{p}} \\
 &= \frac{Kp}{4bt} = \frac{(\Omega K') \cdot p}{4bt} \\
 &= \Omega \cdot \left(\frac{4Gtb}{p^3} \right) \cdot \frac{p}{4bt} \\
 &= \Omega \cdot \frac{p}{p^3} \cdot G
 \end{aligned} \tag{12}$$

Typical results. - Figure 8 shows the typical variation of Ω with respect to b/p , the ratio of semi-length to pitch, for a particular shape of cross section ($f/p = 2e/p = 0.3$, $h/p = 0.3$) and three different values of the sheet thickness-to-pitch ratio, t/p .

It will be noted that as the length-to-pitch ratio increases Ω approaches unity; that is, the stiffness approaches the value associated with continuous attachment of such a nature as to produce a uniform shear strain throughout the sheet. This is to be expected since the discretely attached and the continuously attached plates differ from each other only by a St. Venant effect, that is an effect which is localized near the ends of the corrugations.

The approach of Ω to unity as b/p increases is seen to be much more rapid for the thicker sheets than for the thinner sheets. For

example, at $b/p = 10$ (length-to-pitch ratio of 20), the values of Ω for $t/p = .025$ and $t/p = .005$ are .74 and .15, respectively. It is apparent also that the "end effects" undoubtedly can propagate an appreciable distance inward, especially for the thinner sheets. For example, for $t/p = .005$ and a length-to-pitch ratio as large as 200 ($b/p = 100$), the value of Ω is still only .64, that is the absolute shear stiffness in the case of discrete attachment is only 64 percent of that achievable with continuous attachment.

The curves in figure 8 for the three different values of t/p can be seen to have virtually the same shape and they can therefore be made to nearly coincide if each one is shifted horizontally a different amount. This suggests that t/p can be very nearly eliminated as a parameter by changing the abscissa from b/p to $(b/p) \cdot \phi(t/p)$ where $\phi(t/p)$ is some function of t/p . The effect of such a change, when a logarithmic scale is used for the abscissa, is to shift each curve horizontally as a rigid body a distance $\log \phi(t/p)$, and if the function ϕ is properly chosen, these shifts will be such as to bring the curves for different t/p practically into coincidence.

For the particular cross section considered in figure 8, an appropriate function ϕ is found to be $(t/p)^{1.71}$, and the proper abscissa is then $(b/p) (t/p)^{1.71}$. Figure 9 shows the results obtained by replotting the data of figure 8 using the new abscissa. It is seen that, except for a slight separation at the lower end, the curves for all t/p coincide. In other words, for the given cross-sectional shape, the dimensionless stiffness Ω is essentially a function of $(b/p) (t/p)^{1.71}$, rather than a function of b/p and t/p separately. The advantage of such replotting is that it greatly simplifies, or even eliminates the need for, interpolation and possibly extra-

polution with respect to t/p . Furthermore, it reduces greatly the number of graphs required in presenting the results.

General results. - In figure 10 are plotted the results obtained for all combinations of the cross-sectional shape parameters f/p and h/p . The results are plotted in the economical form discussed above, i.e. by means of semi-logarithmic plots of Ω versus $(b/p)(t/p)^n$, the exponent n being chosen so as to make the curves for different t/p coincide as nearly as possible. As implied in figure 10, the exponent n depends upon f/p , but turns out to be independent of h/p .

Comparing the curves for different h/p values in any one of the four parts of figure 10, it is seen that the smaller h/p (that is, the more nearly we approach a flat plate), the higher the value of Ω . Comparing the four parts of figure 10 with each other, it is evident that reduction of $f/p (=2e/p)$ also leads to an increase in Ω .

Further reductions in the number of parameters. - Examining any one of the four families of curves in figure 10, it can be seen that the curves for different values of h/p differ from each other mainly by a rigid-body horizontal shift. This suggests that another condensation of the results can be effected by properly incorporating h/p into the abscissa. This is done in figure 11, where Ω is plotted as a function of $(b/p)(t/p)^n/(h/p)^m$ for the four different values of f/p . With this abscissa the results for the various combinations of t/p and h/p all lie within the bands shown. The exponent m , like n , is a function of f/p , but a much less sensitive one than n . The numerical values of both exponents appropriate to each band are shown alongside the bands.

A final condensation of the four bands of figure 11 into a single, somewhat wider, band is accomplished by incorporating f/p into the abscissa,

as shown in figure 12. In this figure, if one is willing to neglect the uncertainty represented by the finite width of the band, Ω is given as a function of the single parameter $(b/p) (t/p)^n (h/p)^{-m} (f/p)^{-2.79}$, where n and m are, in turn, functions of f/p . The variation of n and m with f/p is shown by the small inset graph in figure 12. The curves of n and m are shown dotted between f/p of 0.3 and 0.5 because of the uncertainty of the fairing in this region due to the absence of computed data for $f/p = 0.4$.

Figure 11 represents the most economical presentation of the results. It is also the most convenient one for practical use, for it eliminates the need of interpolation with respect to t/p , h/p or f/p , provided that the error due to the finite width of the band is considered acceptable.

Comparison of different end attachment conditions. - Figure 13 illustrates the sensitivity of Ω to the end attachment conditions. It shows, for a particular cross section, the variation of Ω with respect to b/p for three kinds of end attachments. The middle curve is for the present case. The top and bottom curves, taken from reference 1, are for wide attachments to a rigid flange and point attachments with no interfering end member, respectively. It is seen that for the smaller length-to-pitch ratios a large percentage change in Ω is produced in going from one type of attachment to another. For the very long corrugations all the Ω values are close to unity, and there is therefore relatively little change in Ω as a result of altering the end attachment conditions.

ILLUSTRATIVE APPLICATION

In order to illustrate the use of the graphical results presented herein, a particular numerical example will now be considered, involving the corrugated shear web in a hinged picture frame shown in figure 14. The assembly is fastened to a rigid wall along its left side and loaded with a vertical shear of 100 kips at the right end. The web is of steel with a shear modulus, G , of 12,000,000 psi.

The problem is to determine the vertical deflection of the right end. The axial and flexural deformations of the edge members will be assumed to be negligible, and because of the hinges at the corners the entire vertical load will be assumed to be carried by the web alone. It is assumed further that, by means of guides or through proper lateral location of the 100-kip load, the action of the structure is one of pure shearing without twist.

The problem will be separated into two parts: First, the determination of the dimensionless shear stiffness Ω . Second, the conversion of Ω into a dimensional shear stiffness, from which the desired deflection can be obtained.

Determination of Ω . - Figure 12 will first be used for the quickest determination of Ω . To that end the following ratios are needed:

$$\frac{b}{p} = \frac{30}{3} = 10$$

$$\frac{t}{p} = \frac{1/16}{3} = .02080$$

$$\frac{h}{p} = \frac{\sin 60^\circ}{3} = .2887$$

$$\frac{f}{p} = \frac{1}{3} = .3333$$

From the inset graph of figure 12 the following exponent values are obtained for $f/p = .3333$:

$$n = 1.68$$

$$m = 1.48$$

The abscissa required for the use of figure 12 can now be evaluated:

$$\frac{\frac{b}{p} \left(\frac{t}{p}\right)^n}{\left(\frac{h}{p}\right)^m \left(\frac{f}{p}\right)^{2.79}} = \frac{10(.02080)^{1.68}}{(.2887)^{1.48} (.3333)^{2.79}} = 2.01$$

Corresponding to this value of the abscissa, the scatter band of fig. 12 gives Ω as lying between .64 and .70. Selecting the middle of the scatter band, one obtains $\Omega = .67$.

As a check, the value of Ω will now be recomputed by interpolation among the more accurate graphs of figure 10. The required abscissas are as follows:

$$\frac{b}{p} \left(\frac{t}{p}\right)^{1.91} = 10(.02080)^{1.91} = .00613$$

$$\frac{b}{p} \left(\frac{t}{p}\right)^{1.81} = 10(.02080)^{1.81} = .00903$$

$$\frac{b}{p} \left(\frac{t}{p}\right)^{1.71} = 10(.02080)^{1.71} = .0133$$

$$\frac{b}{p} \left(\frac{t}{p}\right)^{1.60} = 10(.02080)^{1.60} = .0204$$

Entering these abscissas into parts (a) through (d) respectively of figure 10, and interpolating with respect to h/p , one obtains the following values of Ω :

$\frac{f}{p}$.1	.2	.3	.5
Ω	.961	.83	.69	.48

Plotting this relationship and putting a smooth curve through the points, one obtains, for $f/p = .3333$, $\Omega = .65$.

The graphs of figure 10 do not contain any scatter bands and are therefore inherently more accurate than figure 12, which suggests that the second value of Ω , namely .65, is more accurate than the first. However, one cannot be certain of this, because figure 10 requires interpolations, which can reduce accuracy.

Computation of vertical deflection of right end. - With $\Omega = .65$ selected as the probably more accurate value, equation (12) gives the following effective shear modulus:

$$\begin{aligned} G_{\text{eff}} &= (.65) \times \frac{3}{4} \times 12,000,000 \\ &= 5,850,000 \text{ psi} \end{aligned}$$

The average shear stress on vertical cross sections is

$$\tau = \frac{100,000}{(60) \left(\frac{1}{16}\right)} = 26,667 \text{ psi}$$

Thus, the overall shear strain angle γ is

$$\gamma = \frac{\tau}{G_{\text{eff}}} = \frac{26,667}{5,850,000} = .00456$$

In a 27-inch length, this leads to a tip deflection of $27 \times (.00456)$, or 0.123 inch.

It should be noted that in this calculation the stiffening effect of the attachments along the two vertical sides of the web is being neglected, because the Ω curves are based on the assumption that the plate is infinitely wide in the direction perpendicular to the direction of the corrugations.

CONCLUDING REMARKS

Theory and curves have been presented for computing the shear stiffness of a trapezoidally corrugated plate attached to relatively rigid flanges by means of small attachments at the ends of the trough lines, in such a way that the flanges interfere with the deformations of the end cross sections of the plate.

The analysis is an approximate one, based on the method of minimum total potential energy, linear elasticity, and the assumption of small deformations. Although the analysis permits a rather general type of cross section, the computed curves are restricted to the case of equal-width crests and troughs.

Experimental data are lacking against which to compare the theor-

etical results. Because of the simplifying assumptions made in the analysis -- assumptions regarding the nature of the deformations, and idealizations regarding the attachments -- it is felt that experimental verification of the theoretical results would be desirable.

APPENDIX I

SOLUTION OF PROBLEM I

In this appendix the solution of the problem represented in figure 6(a) will be described. This problem was solved in reference 1, and therefore most of the mathematical details will here be omitted, except where certain equations can be given in a different form more conducive to computational accuracy.

As mentioned earlier, the plate is assumed to be composed of infinitely many identical corrugations, all deforming in an identical way, and the analysis may therefore be based on a single corrugation, such as the corrugation between trough lines mn and pq of figure 6(a). The shearing of this corrugation is imagined to be effected by a forward longitudinal shift of mn through a distance u_0 and a rearward longitudinal shift of pq through the same distance, producing a total relative shift of $2u_0$ for the corrugation. In these shifts the end points $m, n, p,$ and q of the trough lines are moved only longitudinally. However, the rest of the points of a trough line are permitted to move both longitudinally and laterally, so that the trough lines, as well as all other longitudinal generators, may become curved. Considerations of symmetry and continuity dictate that there can be no vertical displacements of points on the trough lines. These considerations also lead to the conclusions that all the points on a given trough line have the same longitudinal displacement (i.e., the trough lines experience no longitudinal strain) and both trough lines curve into identical shapes.

The analysis is based on certain assumed degrees of freedom for the deformations of the cross sections. These degrees of freedom will be described with the aid of figure 15. Part (a) of that figure shows the middle surface of the cross section and the station numbers assigned for convenience to the edges and the various corners of the cross section. Part (b) shows the assumptions regarding the longitudinal displacements appropriate to the antisymmetrical nature of the deformation. At stations 0 and 5 these displacements are $+u_0$ and $-u_0$, respectively, as already discussed, with u_0 independent of z . At stations 1 and 4 the longitudinal displacements are $+u_1$ and $-u_1$, respectively, with u_1 depending on z ; at stations 2 and 3 they are similarly $+u_2(z)$ and $-u_2(z)$. In between stations, the longitudinal displacements are assumed to vary linearly. Therefore the longitudinal displacements of all middle surface points of the corrugation are defined by one prescribed-displacement parameter u_0 and two unknown functions of z : $u_1(z)$ and $u_2(z)$. If the resultant longitudinal shearing force F , is regarded as prescribed instead of u_0 , the latter becomes an unknown constant.

The deformations of a cross section in its own plane are assumed to be inextensional and to be a superposition of the three antisymmetrical component modes shown in figure 15(c). The third of these modes is a rigid-body horizontal translation of an amount $v_0(z)$. The other two modes are identical with the deformations of a uniform rigid-jointed frame of the same shape as the cross section, with stations 0 and 5 hinged and certain displacements imposed on the joints corresponding to stations 1, 2, 3 and 4. For the first mode shown in figure 15(c)

an upward vertical displacement of an amount $v_1(z)$ is imposed at joint 1, and the same displacement is imposed downward at joint 4, while joint 2 is constrained to slide parallel to line 1-2 and joint 3 is similarly constrained to slide parallel to line 3-4. These sliding displacements must be $v_1 \sin \theta$, as shown in the figure, in order to satisfy the inextensibility assumption. For the second mode shown in figure 15(c) joint 2 is displaced an amount $v_2(z)$ perpendicular to line 1-2, and joint 3 a like amount perpendicular to line 3-4, while joints 1 and 4 are held in their places. In both of the frame-deformation modes of figure 15(c) the joints are permitted to rotate freely as rigid joints. Thus the deformations of all cross sections in their own planes are defined by three unknown functions of z : $v_0(z)$, $v_1(z)$, $v_2(z)$.

On the basis of these assumptions one can now write expressions for the displacement components u , v , w of any point on the middle surface of any plate element in terms of u_0 , $u_1(z)$, $u_2(z)$, $v_0(z)$, $v_1(z)$, and $v_2(z)$. The location of a middle-surface point can be specified by its longitudinal coordinate, z , and its transverse coordinate, s , the latter measured from an edge of the plate element in which the point lies (see fig. 15(a)).

The displacement components u and v are respectively longitudinal (z -wise) and transverse (s -wise). The w displacement component is measured perpendicular to the plate element in which the point lies. The middle surface strains, curvatures, and twist can then be evaluated via the following expressions

$$\text{Longitudinal strain:} \quad \epsilon = \frac{\partial u}{\partial z}$$

$$\text{Shear strain:} \quad \gamma_{sz} = \frac{\partial u}{\partial s} + \frac{\partial v}{\partial z}$$

$$\text{Longitudinal curvature:} \quad \frac{\partial^2 w}{\partial z^2}$$

$$\text{Transverse curvature:} \quad \frac{\partial^2 w}{\partial s^2}$$

$$\text{Twist:} \quad \frac{\partial^2 w}{\partial s \partial z}$$

(By virtue of the inextensibility assumption, the transverse strain $\partial v / \partial s$ of the middle surface is zero). With u , v , and w expressed in terms of the basic degrees of freedom u_0 , $u_1(z)$, ..., $v_2(z)$, the above strains, curvatures, and twist also become functions of these degrees of freedom.

The strain energy of deformation of each plate element can then be written. For this purpose the material is assumed to be isotropic and the strain energy per unit of middle-surface area is taken as

$$\begin{aligned} W = \frac{1}{2} D \left[\left(\frac{\partial^2 w}{\partial z^2} \right)^2 + 2\nu \frac{\partial^2 w}{\partial s^2} \frac{\partial^2 w}{\partial z^2} + \left(\frac{\partial^2 w}{\partial s^2} \right)^2 + 2(1-\nu) \left(\frac{\partial^2 w}{\partial s \partial z} \right)^2 \right] \\ + \frac{1}{2} Et \left(\frac{\partial u}{\partial z} \right)^2 + \frac{1}{2} Gt \left(\frac{\partial u}{\partial s} + \frac{\partial v}{\partial z} \right)^2 \end{aligned} \quad (I-1)$$

where E is Young's modulus, G is the shear modulus, ν is Poisson's ratio, and $D = Et^3 / [12(1-\nu^2)]$. It will be noted that there is a slight inconsistency between the assumption that the transverse strains are zero and the use of E (rather than $E/(1-\nu^2)$) in the term which represents the strain energy density of middle-surface longitudinal deformation, i.e. the term containing $(\partial u / \partial z)^2$. This inconsistency is deliberate; it is felt that in actuality the assumption of

zero transverse stress is more nearly correct than the one of zero transverse strain, and therefore $Et(\partial u/\partial z)^2$ is a better representation of the strain energy density of longitudinal extension than is $[Et/(1-\nu^2)] (\partial u/\partial z)^2$.

In reference 1 two simplifications were made to equation (I-1), and these simplifications were retained in the present analysis of Problem I. The first is the dropping of the underlined terms on the ground that the longitudinal curvatures $\partial^2 w/\partial z^2$ are probably much smaller than the transverse curvatures $\partial^2 w/\partial s^2$.* The second is the replacement of the local twist $\partial^2 w/\partial s \partial z$ by the average twist over the width of the plate element. For example, for the plate element 0-1, the twist was assumed constant across the width at the value $d(v_1/e)/dz$. The twist makes only a small contribution to the total strain energy, and its approximate treatment in this fashion should introduce very little error.

With these simplifications made, and w , u and v expressed in terms of u_0 , $u_1(z)$, ..., $v_2(z)$, the strain-energy density W becomes a function of these six parameters. The strain energy of one of the plate elements can be written as a double integral of W over the area of the plate element, and the integration with respect to the s -coordinate can be carried out explicitly. The total strain energy U is obtained by summing the strain energies of the five individual

*We point out in advance that this simplification will not be permissible in appendix II.

plate elements. The total potential energy (TPE) is obtained by adding the potential energy $-F_1 \cdot 2u_0$ of the applied shear loads to the strain energy U . The resulting expression for the TPE is equation (A1) of reference 1, in which the symbol F would be F_1 in the present notation.*

The expression for the TPE thus obtained is a functional of $u_0, u_1(z), \dots, v_2(z)$. By means of the variational calculus, differential equations, boundary conditions, and one integral equation are obtained defining those $u_0, u_1(z), \dots, v_2(z)$ which minimize the total potential energy and which therefore represent the "best" approximate solution to the problem within the framework of the permitted degrees of freedom of deformation. In taking the first variation of the TPE use must be made of the *a priori* boundary conditions of constraint, namely $v_0(\pm b) = 0$.

The differential equations and boundary conditions to be solved are linear, and the details of their solution may be found in appendix B of reference 1 and will not be repeated here. However, we will take the opportunity here to note that better computational accuracy can be achieved by using different expressions than in reference 1 for the coefficients of the characteristic equation. This characteristic equation (B12 of ref. 1) is

$$(k_0 + k_2 r^2 + k_4 r^4 + k_6 r^6 + k_8 r^8) r^2 = 0 \quad (I-2)$$

and it is to be solved for the roots r_1, r_2, \dots, r_{10} . The coefficients are defined by equations (B 13) of reference 1, but the following equivalent definitions require fewer arithmetic operations and were therefore used instead**:

*The procedure used in reference 1 in order to obtain the TPE is described therein in a somewhat different way, but it is actually equivalent to the procedure given above.

**The k_0, \dots, k_8 definitions given here also differ by a constant factor from the ones₀ given in reference 1; since the right side of equation (I-2) is zero, this difference will not affect the roots.

$$\begin{aligned}
k_0 &= CGQ_1 + D_8P_1D_5 + D_3JM - GD_5M - CJP_1 - D_8D_3Q_1 \\
k_2 &= BGQ_1 + CFQ_1 + D_7P_1D_5 + D_8(N_1D_5 + P_1D_4) + D_2JM \\
&\quad + D_3(MH + JK) - FD_5M - G(D_5K + D_4M) - BJP_1 \\
&\quad - C(JN_1 + HP_1) - D_7D_3Q_1 - D_8D_2Q_1 \\
k_4 &= AGQ_1 + CEQ_1 + BFQ_1 + D_6P_1D_5 + D_8N_1D_4 + D_7(N_1D_5 + P_1D_4) \\
&\quad + D_1JM + D_3KH + D_2(MH + JK) - ED_5M - GD_4K \\
&\quad - F(D_5K + D_4M) - AJP_1 - CHN_1 - B(JN_1 + HP_1) \\
&\quad - D_6D_3Q_1 - D_8D_1Q_1 - D_7D_2Q_1 \\
k_6 &= AFQ_1 + BEQ_1 + D_7N_1D_4 + D_6(N_1D_5 + P_1D_4) + D_2KH \\
&\quad + D_1(MH + JK) - FD_4K - E(D_5K + D_4M) - A(JN_1 + HP_1) \\
&\quad - BHN_1 - D_6D_2Q_1 - D_7D_1Q_1 \\
k_8 &= AEQ_1 + D_6N_1D_4 + D_1KH - ED_4K - AHN_1 - D_6D_1Q_1
\end{aligned}
\tag{I-3}$$

where

$$\begin{aligned}
A &= -\frac{1}{2} b_{11}e_{10}d_{22} + \frac{1}{2} (b_{11}d_{20} - b_{12}d_{10}) e_{12} \\
B &= -\frac{1}{2} \left(\frac{1}{4} d_{10}d_{11} - c_{11}e_{10} \right) d_{22} - \frac{1}{2} a_{12} (b_{11}d_{20} - b_{12}d_{10}) \\
&\quad + \frac{1}{2} e_{12} (c_{12}d_{10} - c_{11}d_{20}) \\
C &= -\frac{1}{2} a_{12} (c_{12}d_{10} - c_{11}d_{20}) \\
D_1 &= -\frac{1}{2} d_{22}b_{12}e_{10} + \frac{1}{2} (b_{12}d_{20} - b_{22}d_{10}) e_{12} \\
D_2 &= \frac{1}{2} (e_{10}c_{12} - \frac{1}{4} d_{10}d_{21}) d_{22} - \frac{1}{2} a_{12} (b_{12}d_{20} - b_{22}d_{10}) \\
&\quad + \frac{1}{2} e_{12} (c_{22}d_{10} - c_{12}d_{20})
\end{aligned}
\tag{I-4}$$

(equations continued
on next page)

$$D_3 = \frac{1}{2} a_{12} (c_{12}d_{20} - c_{22}d_{10})$$

$$D_4 = \frac{1}{4} (e_{10}d_{11} - e_{11}d_{10}) d_{22} + \frac{1}{4} (d_{21}d_{10} - d_{20}d_{11}) e_{12}$$

$$D_5 = \frac{1}{4} a_{11}d_{10}d_{22} - \frac{1}{4} (d_{21}d_{10} - d_{20}d_{11}) a_{12}$$

$$D_6 = -\frac{1}{2} d_{22}e_{20}b_{11} + \frac{1}{2} e_{22} (d_{20}b_{11} - d_{10}b_{12})$$

$$D_7 = \frac{1}{2} d_{22}e_{20}c_{11} - \frac{1}{2} a_{22} (d_{20}b_{11} - d_{10}b_{12}) + \frac{1}{2} e_{22} (c_{12}d_{10} - d_{20}c_{11})$$

$$D_8 = \frac{1}{2} a_{22} (d_{20}c_{11} - c_{12}d_{10})$$

$$E = -\frac{1}{2} e_{20}b_{12}d_{22} + \frac{1}{2} e_{22} (d_{20}b_{12} - b_{22}d_{10})$$

$$F = -\frac{1}{2} d_{22} \left(\frac{1}{4} d_{22}d_{10} - e_{20}c_{12} \right) - \frac{1}{2} a_{22} (d_{20}b_{12} - b_{22}d_{10}) \\ + \frac{1}{2} e_{22} (c_{22}d_{10} - d_{20}c_{12})$$

$$G = -\frac{1}{2} a_{22} (c_{22}d_{10} - d_{20}c_{12})$$

$$H = \frac{1}{4} d_{22} (e_{20}d_{11} - d_{10}e_{12}) - \frac{1}{4} e_{22} (d_{20}d_{11} - d_{21}d_{10})$$

$$J = \frac{1}{4} a_{12}d_{10}d_{22} + \frac{1}{4} a_{22} (d_{20}d_{11} - d_{21}d_{10})$$

$$K = -\frac{1}{2} e_{00}b_{11}d_{22} + \frac{1}{2} e_{20} (d_{20}b_{11} - d_{10}b_{12})$$

$$M = -\frac{1}{2} d_{22} \left(\frac{1}{4} d_{10}^2 - e_{00}c_{11} \right) + \frac{1}{2} e_{20} (c_{12}d_{10} - d_{20}c_{11})$$

$$N_1 = -\frac{1}{2} e_{00}b_{12}d_{22} + \frac{1}{2} e_{20} (d_{20}b_{12} - b_{22}d_{10})$$

$$P_1 = \frac{1}{2} d_{22} (e_{00}c_{12} - \frac{1}{4} d_{20}d_{10}) + \frac{1}{2} e_{20} (c_{22}d_{10} - d_{20}c_{12})$$

$$Q_1 = \frac{1}{4} (e_{00}d_{11}d_{22} - e_{10}d_{10}d_{22} + d_{21}d_{10}e_{20} - d_{20}d_{11}e_{20})$$

The lower case symbols b_{11} , e_{10} , etc. in the above have the same definitions as in reference 1.

Once the differential equations have been solved for $u_1(z), \dots, v_2(z)$ in terms of u_0 , the influence coefficient α_1 depicted in figure 6(a) can be evaluated by equating $\alpha_1 u_0$ to $v_1(b)$. The one integral equation obtained from the variational process relates F_1 and u_0 and therefore yields the stiffness K_1 shown in figure 6(a).

APPENDIX II

SOLUTION OF PROBLEM II

Assumed displacements. - In this appendix the problem depicted in figure 7(a) is analyzed. Again certain modes of deformation are assumed, this time modes which are consistent with the symmetry of the loading and structure and the continuity of each corrugation with its neighbors.

The displacements of a cross section in its own plane are assumed to be a superposition of the two modes shown in figure 16(c). The first is a rigid-body upward translation of an amount $v_0(z)$. The second is the known elastic curve assumed by a uniform inextensible rigid-jointed frame of the same shape as the cross section when the joints 0 and 5 are clamped and joints 1 and 4 are displaced upward an amount $v_1(z)$, and all the joints except 0 and 5 are permitted to rotate freely as rigid joints. Thus the displacements of any cross section in its own plane are defined by two unknown functions of z : $v_0(z)$ and $v_1(z)$.

Figure 16(b) shows the assumptions regarding the longitudinal (z -wise) displacements of the middle-surface points of the cross section. As before, these displacements are assumed to vary linearly between stations. At stations 0 and 5 they are equal, by symmetry, and their common value is denoted by $u_0(z)$. As shown in figure 16(b), the displacements at the adjacent stations, 1 and 4, are also taken as $u_0(z)$. This is done because symmetry dictates that there be no transference of shear flow across the trough lines from one corrugation to the next;

hence the shear strain in the plate elements 0-1 and 4-5 must be zero. At stations 2 and 3 the common longitudinal displacement is designated as μ times $u_o(z)$, where μ is a constant so chosen as to give zero for the mean longitudinal displacement over the entire cross section, in accordance with the requirement of zero resultant tension or compression on the cross section.* The required value of μ is readily determined to be

$$\mu = - \frac{2e+k}{f+k} \quad (\text{II-1})$$

For the case of equal-width crests and troughs, $\mu=-1$. Thus a single unknown function, $u_o(z)$, defines the longitudinal displacements of all middle-surface points of the corrugation.

Longitudinal strains. - From figure 16(b) the following expressions are readily obtained for the longitudinal strains ϵ of the middle surface of plate elements 0-1, 1-2, and 2-3:

Plate element	Longitudinal strain, ϵ
0-1	$\frac{du_o}{dz}$
1-2	$\frac{du_o}{dz} + \frac{s}{k} (\mu-1) \frac{du_o}{dz}$
2-3	$\mu \frac{du_o}{dz}$

(II-2)

The coordinate s is measured from the left side of the plate element, as shown in figure 16(a). The strains for the plate elements 3-4 and 4-5 can be obtained from symmetry.

*See section entitled "Statement of problem" under METHOD OF ANALYSIS.

Shear strains. - Figures 16(b) and (c) give the following expressions for the middle-surface shear strains γ :

Plate element	Shear strain, γ
0-1	0
1-2	$\frac{d}{dz} (v_o \sin\theta + v_1 \sin\theta) + \frac{(\mu-1)u_o}{k}$
2-3	0

(II-3)

Normal displacements. - The displacements normal to the plate elements will be denoted by $w_1(s,z)$, $w_2(s,z)$, etc. (When it is not important to identify the particular plate element under consideration, the symbol w , without a subscript, will be used to denote normal displacement.) The positive directions of w_1 , w_2 , etc. are shown in figure 16(a). Equations for these displacements can be obtained by making an elastic analysis of the rigid-jointed frame corresponding to the bottom diagram of figure 16, and then adding on the normal displacements due to the rigid-body translation $v_o(z)$. The resulting expressions are:

$$\begin{aligned}
 w_1 &= v_o + v_1 \left[\left(\frac{s}{e}\right)^2 \beta_{12} + \left(\frac{s}{e}\right)^3 \beta_{13} \right] \\
 w_2 &= v_o \cos\theta + v_1 \left[\cos\theta + \frac{s}{k} \beta_{21} + \left(\frac{s}{k}\right)^2 \beta_{22} + \left(\frac{s}{k}\right)^3 \beta_{23} \right] \\
 w_3 &= v_o + v_1 \left[1 + \frac{s}{f} \beta_{31} + \left(\frac{s}{f}\right)^3 \beta_{32} \right]
 \end{aligned}
 \tag{II-4}$$

where

$$\begin{aligned}
\beta_{12} &= 3 \left[1 - \frac{1}{\beta} \frac{p}{e} \left(2\frac{f}{k} + 1 \right) \right] \\
\beta_{13} &= -2 + \frac{3}{\beta} \frac{p}{e} \left(2\frac{f}{k} + 1 \right) \\
\beta_{21} &= \frac{3}{\beta} \frac{k}{e} \frac{p}{e} \left(2\frac{f}{k} + 1 \right) \\
\beta_{22} &= -\frac{3}{\beta} \frac{k}{e} \frac{p}{e} \left(3\frac{f}{k} + 2 \right) \\
\beta_{23} &= \frac{3}{\beta} \frac{k}{e} \frac{p}{e} \left(\frac{f}{k} + 1 \right) \\
\beta_{31} &= -\frac{3}{\beta} \frac{f^2 p}{e^2 k} \\
\beta_{32} &= -\beta_{31}
\end{aligned} \tag{II-5}$$

with

$$\beta \equiv 3 \frac{pf}{k^2} + 4 \frac{pf}{ek} + 2 \frac{p}{k} + 2 \frac{p}{e} \tag{II-6}$$

Expressions for the curvatures and twist of the middle surface can be readily obtained from equations (II-4). For example, for plate element 0-1 they are:

$$\begin{aligned}
\frac{\partial^2 w_1}{\partial z^2} &= \frac{d^2 v_0}{dz^2} + \frac{d^2 v_1}{dz^2} \cdot \left[\left(\frac{s}{e} \right)^2 \beta_{12} + \left(\frac{s}{e} \right)^3 \beta_{13} \right] \\
\frac{\partial^2 w_1}{\partial s^2} &= v_1 \cdot \left[\frac{2}{e^2} \beta_{12} + \frac{6s}{e^3} \beta_{13} \right] \\
\frac{\partial^2 w_1}{\partial s \partial z} &= \frac{dv_1}{dz} \cdot \left[\frac{2s}{e^2} \beta_{12} + \frac{3s^2}{e^3} \beta_{13} \right]
\end{aligned} \tag{II-7}$$

Strain energy. - Assuming an isotropic linearly elastic material, the strain energy of any plate element per unit of middle-surface area can be written as in Appendix I, namely

$$W = \frac{1}{2} D \left[\left(\frac{\partial^2 w}{\partial z^2} \right)^2 + 2\nu \frac{\partial^2 w}{\partial s^2} \frac{\partial^2 w}{\partial z^2} + \left(\frac{\partial^2 w}{\partial s^2} \right)^2 + 2(1-\nu) \left(\frac{\partial^2 w}{\partial s \partial z} \right)^2 \right] \\ + \frac{1}{2} E t \epsilon^2 + \frac{1}{2} G t \gamma^2 \quad (\text{II-8})$$

where w , ϵ and γ are the normal displacement, longitudinal strain, and shear strain appropriate to the particular plate element under consideration, from equations (II-2), (II-3) and (II-4). Trial analyses have shown that serious error results if the terms containing $\partial^2 w / \partial z^2$ are neglected here as they were in Appendix I. Accordingly all the terms shown in the above equation will be retained in the further development of this appendix.

The total strain energy of any plate element can be written as an integral of W over the entire length and width of the plate element; i.e.

$$\int_{-b}^b \int_0^a W \, ds \, dz \quad (\text{II-9})$$

where a is the width of the particular plate element under consideration ($a=e$, k , or f). Substituting the appropriate expressions for w , ϵ , and γ , the integration with respect to s can be carried out explicitly, leaving only an integral with respect to z . If this is done for each of the five plate elements, and the resulting five strain energies are summed, the following expression is obtained for the total strain energy U of the entire corrugation:

$$U = \int_{-b}^b (V_{sh} + V_e + V_f) \, dz \quad (\text{II-10})$$

where V_{sh} , V_e , V_f are respectively the strain energies of middle-surface shear, middle-surface extension, and plate flexure and twisting, per unit length of corrugation, and are given by the following expressions:

$$V_{sh} = Gtp \left[(1-\mu)^2 \left(\frac{u_o}{p} \right)^2 \frac{p}{k} + 2(\mu-1) \sin\theta \cdot \frac{u_o}{p} \left(\frac{dv_o}{dz} + \frac{dv_1}{dz} \right) + \frac{k}{p} \sin^2\theta \left(\frac{dv_o}{dz} + \frac{dv_1}{dz} \right)^2 \right] \quad (II-11)$$

$$V_e = Etp \left(\frac{du}{dz} \right)^2 \left[\frac{e}{p} + \frac{1}{3} (1+\mu+\mu^2) \frac{k}{p} + \frac{1}{2} \mu^2 \frac{f}{p} \right] \quad (II-12)$$

$$V_f = \frac{Dv_1^2}{p^3} \cdot \alpha_1 + \frac{D}{p} \left(\frac{dv_1}{dz} \right)^2 \cdot 6(1-\nu) \alpha_2 + D \left[p \left(\frac{d^2v_o}{dz^2} \right)^2 \alpha_3 + 2p \frac{d^2v_o}{dz^2} \frac{d^2v_1}{dz^2} \alpha_4 + p \left(\frac{d^2v_1}{dz^2} \right)^2 \alpha_5 + \frac{2\nu}{p} v_1 \frac{d^2v_o}{dz^2} \alpha_6 + \frac{2\nu}{p} v_1 \frac{d^2v_1}{dz^2} \alpha_7 \right] \quad (II-13)$$

where

$$\begin{aligned} \alpha_1 &= \left(\frac{p}{e} \right)^3 (4\beta_{12}^2 + 12\beta_{12}\beta_{13} + 12\beta_{13}^2) \\ &\quad + \left(\frac{p}{k} \right)^3 (4\beta_{22}^2 + 12\beta_{22}\beta_{23} + 12\beta_{23}^2) + \frac{18}{\beta^2} \frac{p^5 f}{e^4 k^2} \\ \alpha_2 &= \frac{p}{e} \left(\frac{4}{9} \beta_{12}^2 + \beta_{12}\beta_{13} + \frac{3}{5} \beta_{13}^2 \right) \\ &\quad + \frac{p}{k} \left(\frac{1}{3} \beta_{21}^2 + \frac{2}{3} \beta_{21}\beta_{22} + \frac{2}{3} \beta_{21}\beta_{23} + \frac{4}{9} \beta_{22}^2 + \beta_{22}\beta_{23} + \frac{3}{5} \beta_{23}^2 \right) \\ &\quad + \frac{7}{10} \frac{1}{\beta^2} \frac{p^3 f^3}{e^4 k^2} \\ \alpha_3 &= \frac{e}{p} + \frac{k}{p} \cos^2\theta + \frac{1}{2} \frac{f}{p} \end{aligned} \quad (II-14)$$

(equations continued on next page)

$$\alpha_4 = \frac{e}{p} \left(\frac{1}{3} \beta_{12} + \frac{1}{4} \beta_{13} \right) + \frac{k}{p} \left(\cos\theta + \frac{1}{2} \beta_{21} + \frac{1}{3} \beta_{22} + \frac{1}{4} \beta_{23} \right) \cos\theta \\ + \frac{1}{2} \frac{f}{p} \left(1 + \frac{1}{2} \beta_{31} + \frac{1}{3} \beta_{32} \right)$$

$$\alpha_5 = \frac{e}{p} \left(\frac{1}{5} \beta_{12}^2 + \frac{1}{3} \beta_{12}\beta_{13} + \frac{1}{7} \beta_{13}^2 \right) \\ + \frac{k}{p} \left[\cos^2\theta + 2\cos\theta \left(\frac{1}{2} \beta_{21} + \frac{1}{3} \beta_{22} + \frac{1}{4} \beta_{23} \right) + \frac{1}{3} \beta_{21}^2 \right. \\ \left. + \frac{1}{2} \beta_{21}\beta_{22} + \frac{1}{5} \beta_{22}^2 + \frac{2}{5} \beta_{21}\beta_{23} + \frac{1}{3} \beta_{22}\beta_{23} + \frac{1}{7} \beta_{23}^2 \right] \\ + \frac{1}{2} \frac{f}{p} \left(1 + \beta_{31} + \frac{1}{3} \beta_{31}^2 + \frac{2}{3} \beta_{32} + \frac{1}{2} \beta_{31}\beta_{32} + \frac{1}{5} \beta_{32}^2 \right)$$

$$\alpha_6 = \frac{p}{e} (2\beta_{12} + 3\beta_{13}) + \frac{p}{k} (2\beta_{22} + 3\beta_{23}) \cos\theta + \frac{p}{f} \beta_{32}$$

$$\alpha_7 = \frac{p}{e} \left(\frac{2}{3} \beta_{12}^2 + 2\beta_{12}\beta_{13} + \frac{6}{5} \beta_{13}^2 \right) \\ + \frac{p}{k} \left[(2\beta_{22} + 3\beta_{23}) \cos\theta + \beta_{22}\beta_{21} + 2\beta_{23}\beta_{21} \right. \\ \left. + \frac{2}{3} \beta_{22}^2 + 2\beta_{23}\beta_{22} + \frac{6}{5} \beta_{23}^2 \right] \\ + \frac{p}{f} \beta_{32} \left(1 + \frac{1}{2} \beta_{31} + \frac{1}{3} \beta_{32} \right)$$

In the above equation for V_f , the α_1 term represents those contributions arising from the term $(\partial^2 w / \partial s^2)^2$ in equation (II-8); the α_2 term those due to $(\partial^2 w / \partial s \partial z)^2$; the α_3 , α_4 and α_5 terms those coming from $(\partial^2 w / \partial z^2)^2$; and the α_6 and α_7 terms those due to $(\partial^2 w / \partial s^2) (\partial^2 w / \partial z^2)$.

Total potential energy. - The total potential energy (TPE) of a single corrugation is obtained by adding to the strain energy U (eq. (II-10)):

the potential energy $-4P[v_1(b) + v_0(b)]$ of the applied loads on one corrugation (See figs. 7(a) and 16). The attachments at the ends of the trough lines require that the vertical deflection at stations 0 and 5 of the end cross sections be zero. Referring to figure 16(c), this implies the geometric boundary condition

$$v_0(\pm b) = 0 \quad (\text{II-15})$$

Thus the potential energy of the applied loads can be written simply as $-4Pv_1(b)$, and the TPE is therefore

$$\text{TPE} = U - 4Pv_1(b) \quad (\text{II-16})$$

Minimization of the TPE. - The TPE (eq. (II-16)) is a functional of $u_0(z)$, $v_0(z)$, and $v_1(z)$. We now seek the forms of these functions which minimize the TPE. To that end we first form the first variation of the TPE, $\delta(\text{TPE})$, due to the variations $\delta u_0(z)$, $\delta v_0(z)$, $\delta v_1(z)$ in $u_0(z)$, $v_0(z)$ and $v_1(z)$, by the standard technique of the variational calculus. In the resulting expression any integrands containing derivatives of δu_0 , δv_0 , or δv_1 can be reduced through integration by parts to integrands that involve δu_0 , δv_0 , δv_1 alone, rather than their derivatives. Performing such integrations by parts, taking into account the boundary condition equation (II-15), the even-ness of v_0 and v_1 with respect to z , and the oddness of u_0 with respect to z , one obtains

$$\frac{1}{D} \cdot \delta(\text{TPE}) = \int_{-b}^b [L_{v_0} \cdot \delta v_0(z) + L_{v_1} \cdot \delta v_1(z) - L_{u_0} \cdot \frac{\delta u_0(z)}{p}] dz$$

$$\begin{aligned}
& + 4K \cdot B_{u_0} \frac{1}{p} \delta u_0(b) \\
& + 4B'_{v_0} \left[\frac{d(\delta v_0)}{dz} \right]_{z=b} + 4B'_{v_1} \left[\frac{d(\delta v_1)}{dz} \right]_{z=b} \\
& - \left(\frac{4P}{D} + B_{v_1} \right) \delta v_1(b)
\end{aligned} \tag{II-17}$$

where

$$\begin{aligned}
L_{v_0} & \equiv \left[2\alpha_3 p \frac{d^4 v_0}{dz^4} - \frac{K_2 g_{10}}{p} \frac{d^2 v_0}{dz^2} \right] \\
& + \left[2\alpha_4 p \frac{d^4 v_1}{dz^4} + \left(2\alpha_6 \frac{v}{p} - \frac{K_2 g_{10}}{p} \right) \frac{d^2 v_1}{dz^2} \right] \\
& + \left[(1-\mu) K_2 \frac{g_8}{p^2} \frac{du_0}{dz} \right]
\end{aligned} \tag{II-18}$$

$$\begin{aligned}
L_{v_1} & \equiv \left[2\alpha_4 p \frac{d^4 v_0}{dz^4} + \left(2\alpha_6 \frac{v}{p} - \frac{K_2 g_{10}}{p} \right) \frac{d^2 v_0}{dz^2} \right] \\
& + \left[2\alpha_5 p \frac{d^4 v_1}{dz^4} + \left(4\alpha_7 \frac{v}{p} - \frac{2K_2 g_9}{p} \right) \frac{d^2 v_1}{dz^2} + \frac{2\alpha_1}{p^3} v_1 \right] \\
& + \left[(1-\mu) K_2 \frac{g_8}{p^2} \frac{du_0}{dz} \right]
\end{aligned} \tag{II-19}$$

$$\begin{aligned}
L_{u_0} & \equiv \left[(1-\mu) K_2 \frac{g_8}{p} \frac{dv_0}{dz} \right] \\
& + \left[(1-\mu) K_2 \frac{g_8}{p} \frac{dv_1}{dz} \right] \\
& + \left[2K_1 (2g_1 + g_2 + \mu g_3 + \mu^2 g_4) \frac{d^2 u_0}{dz^2} + K_2 \{g_5 - 2g_6 + \mu g_7 (2-\mu)\} \frac{u_0}{p^2} \right]
\end{aligned} \tag{II-20}$$

$$B_{u_0} \equiv \left(\frac{du_0}{dz} \right)_{z=b} \tag{II-21}$$

$$B'_{v_0} \equiv (\alpha_3 p \frac{d^2 v_0}{dz^2} + \alpha_4 p \frac{d^2 v_1}{dz^2} + \alpha_6 \frac{v}{p} v_1)_{z=b} \quad (II-22)$$

$$B'_{v_1} \equiv (\alpha_4 p \frac{d^2 v_0}{dz^2} + \alpha_5 p \frac{d^2 v_1}{dz^2} + \alpha_7 \frac{v}{p} v_1)_{z=b} \quad (II-23)$$

$$B_{v_1} \equiv [2K_2 \{g_8 (1-\mu) \frac{u_0}{p^2} - \frac{2g_9}{p} \frac{dv_1}{dz} - \frac{g_{10}}{p} \frac{dv_0}{dz}\} + 4 \frac{d}{dz} (\alpha_4 p \frac{d^2 v_0}{dz^2} + \alpha_5 p \frac{d^2 v_1}{dz^2} + \alpha_7 \frac{v}{p} v_1)]_{z=b} \quad (II-24)$$

$$K \equiv K_1 \cdot (2g_1 + g_2 + \mu g_3 + \mu^2 g_4) \quad (II-25)$$

with

$$K_1 \equiv Etp^2/D \quad (II-26)$$

$$K_2 \equiv Gtp^2/D$$

$$g_1 \equiv \frac{1}{3} \frac{e}{p}$$

$$g_2 \equiv \frac{1}{3} (\frac{e}{p} + \frac{k}{p})$$

$$g_3 \equiv \frac{1}{3} \frac{k}{p}$$

$$g_4 \equiv \frac{1}{3} \frac{k}{p} + \frac{1}{2} \frac{f}{p}$$

$$g_5 \equiv 2 \frac{p}{e} \quad (II-27)$$

$$g_6 \equiv \frac{p}{e} + \frac{p}{k}$$

$$g_7 \equiv 2 \frac{p}{k}$$

$$g_8 \equiv 2 \sin \theta$$

$$g_9 \equiv \frac{k}{p} \sin^2 \theta + \alpha_2 (\frac{t}{p})^2$$

$$g_{10} \equiv 2 \frac{k}{p} \sin^2 \theta$$

In order for the TPE to be a minimum, $\delta(\text{TPE})$ must be zero for all variations $\delta v_0(z)$, $\delta v_1(z)$, $\delta u_0(z)$. Therefore v_0 , v_1 and u_0 must satisfy the following differential equations.

$$L_{v_0} = 0, \quad L_{v_1} = 0, \quad L_{u_0} = 0 \quad (\text{II-28})$$

and the following boundary conditions:

$$B_{u_0} = 0, \quad B'_{v_0} = 0, \quad B'_{v_1} = 0, \quad B_{v_1} = -\frac{4P}{D} \quad (\text{II-29})$$

In addition to these, the boundary condition (II-15) arising from the attachments at the ends of the trough lines must be satisfied.

Solution of differential equations. - The differential equations (II-28) and boundary conditions (II-29) and (II-15) are linear, and their solution can therefore be obtained by standard means. Because of the required even-ness of $v_0(z)$ and $v_1(z)$ and oddness of $u_0(z)$, solutions may be sought in the form

$$\begin{aligned} v_0 &= A \cosh(mz/p) \\ v_1 &= B \cosh(mz/p) \\ u_0 &= C \sinh(mz/p) \end{aligned} \quad (\text{II-30})$$

Substitution into the differential equations (II-28) leads to the following characteristic equation defining the admissible values of m :

$$m^2(h_0 + h_2 m^2 + h_4 m^4 + h_6 m^6) = 0 \quad (\text{II-31})$$

where

$$\begin{aligned} h_0 &\equiv K_2 u_2 u_4 - 4\alpha_1 K_1 K_2 g_{10} u_1 + u_5 u_6 \\ h_2 &\equiv 2K_2 u_2 u_3 + 2K_1 u_1 u_4 + 2(2\alpha_4 - \alpha_5 - \alpha_3) u_5 \\ h_4 &\equiv 4(\alpha_3 \alpha_5 - \alpha_4^2) u_2 K_2 + 4u_1 K_1 u_3 \\ h_6 &\equiv 8(\alpha_3 \alpha_5 - \alpha_4^2) u_1 K_1 \end{aligned} \quad (\text{II-32})$$

with

$$\begin{aligned}
u_1 &\equiv 2g_1 + g_2 + \mu g_3 + \mu^2 g_4 \\
u_2 &\equiv g_5 - 2g_6 + \mu g_7 (2-\mu) \\
u_3 &\equiv 2\alpha_3 (2\alpha_7 v - K_2 g_9) + K_2 g_{10} (2\alpha_4 - \alpha_5) - 4v\alpha_4 \alpha_6 \\
u_4 &\equiv 4\alpha_1 \alpha_3 - K_2 g_{10} (4\alpha_7 v - 2K_2 g_9) - (2\alpha_6 v - K_2 g_{10})^2 \\
u_5 &\equiv [(1-\mu) K_2 g_8]^2 \\
u_6 &\equiv 4\alpha_6 v - K_2 g_{10} - 4\alpha_7 v + 2K_2 g_9
\end{aligned} \tag{II-33}$$

The roots of the characteristic equation will be denoted by

$$m = \pm 0, \pm m_2, \pm m_3, \pm m_4 \tag{II-34}$$

The presence of the repeated zero root indicates the existence of a solution not of the form of equations (II-30). By inspection, this solution is found to be

$$\begin{aligned}
v_o &= \gamma_1 B_1 \left(\frac{z}{p}\right)^2 \\
v_1 &= B_1 \\
u_o &= \lambda_1 B_1 \left(\frac{z}{p}\right)
\end{aligned} \tag{II-35}$$

where B_1 is an arbitrary constant and γ_1 and λ_1 have the following definitions:

$$\begin{aligned}
\gamma_1 &= -\frac{\alpha_1}{2v\alpha_6} \\
\lambda_1 &= -\frac{\alpha_1 g_{10}}{(1-\mu) \alpha_6 v g_8} = \frac{\alpha_1 (1-\mu) g_8}{\alpha_6 v u_2}
\end{aligned} \tag{II-36}$$

Adding to the special solution those solutions which are of the form (II-30), one obtains the following complete solution of the differential equations (II-28):

$$v_o = A_o + \gamma_1 B_1 \left(\frac{z}{p}\right)^2 + \gamma_2 B_2 \cosh(m_2 \frac{z}{p}) + \gamma_3 B_3 \cosh(m_3 \frac{z}{p}) + \gamma_4 B_4 \cosh(m_4 \frac{z}{p})$$

$$v_1 = 0 + B_1 + B_2 \cosh(m_2 \frac{z}{p}) + B_3 \cosh(m_3 \frac{z}{p}) + B_4 \cosh(m_4 \frac{z}{p}) \quad (\text{II-37})$$

$$u_o = 0 + \lambda_1 B_1 \left(\frac{z}{p}\right) + \lambda_2 B_2 \sinh(m_2 \frac{z}{p}) + \lambda_3 B_3 \sinh(m_3 \frac{z}{p}) + \lambda_4 B_4 \sinh(m_4 \frac{z}{p})$$

where γ_1 and λ_1 have already been defined, and the remaining γ 's and λ 's are defined by

$$\gamma_i = - \frac{\begin{vmatrix} a_{12} & a_{13} \\ a_{22} & a_{23} \end{vmatrix}}{\begin{vmatrix} a_{11} & a_{13} \\ a_{21} & a_{23} \end{vmatrix}} \quad (i = 2, 3, 4) \quad (\text{II-38})$$

$$\lambda_i = - \frac{\begin{vmatrix} a_{11} & a_{12} \\ a_{21} & a_{22} \end{vmatrix}}{\begin{vmatrix} a_{11} & a_{13} \\ a_{21} & a_{23} \end{vmatrix}} \quad (i = 2, 3, 4) \quad (\text{II-39})$$

where

$$\begin{aligned} a_{11} &= 2\alpha_3 m_i^4 - K_2 g_{10} m_i^2 \\ a_{12} &= a_{21} = 2\alpha_4 m_i^4 + (2\alpha_6 v - K_2 g_{10}) m_i^2 \\ a_{13} &= (1-\mu) K_2 g_8 m_i \\ a_{22} &= 2\alpha_5 m_i^4 + (4\alpha_7 v - 2K_2 g_9) m_i^2 + 2\alpha_1 \\ a_{23} &= a_{13} \end{aligned} \quad (\text{II-40})$$

The five arbitrary constants A_0, B_1, \dots, B_4 are determined in terms of P through the five boundary conditions (II-29) and (II-15), in a straightforward manner.

With these constants known, the deformations are completely determined in terms of P , and one can readily obtain the constant C_3 of figure 7(a) from the equation

$$C_3 P = v_0(b) + v_1(b) = v_1(b) . \quad (\text{II-41})$$

$v_1(b)$ will be proportional to P , and the common factor P will cancel out of equation (II-41).

APPENDIX III

SOLUTION OF PROBLEM III

Problem III (that is, the problem represented by figure 7(b)) possesses the same antisymmetry characteristics as problem I (fig. 6(a)). Its solution can therefore be effected by making only minor changes in the procedure used for solving problem I. The same deformation modes are assumed as for problem I (see fig. 15), except that u_0 is set identically equal to zero, because of the enforced condition of zero overall shear strain in problem III. Consequently, the strain energy functional U for problem III is that of problem I with u_0 set equal to zero. The potential energy of the applied loads for problem III is $+4P v_1(b)$ (see figs. 7(b) and 15), instead of $-F_1 \cdot 2u_0$ as in problem I. The total potential energy functional to be employed in the solution of problem III is therefore

$$\text{TPE} = U + 4P v_1(b) \quad (\text{III-1})$$

In deriving the expression for U the same strain-energy-density expression was used as in problem I (see eq. (I-1)), with the underlined terms again omitted, and the local twist $\partial^2 w / \partial s \partial z$ at any point in a plate element replaced by an average twist across the width of the element.

The minimization of the TPE through the calculus of variations leads to the following differential equations:

$$\begin{aligned}
b_{11} \frac{d^2 u_1}{dz^2} + b_{12} \frac{d^2 u_2}{dz^2} - \frac{1}{2} d_{10} \frac{dv_0}{dz} - \frac{1}{2} d_{11} \frac{dv_1}{dz} - c_{11} u_1 - c_{12} u_2 &= 0 \\
b_{12} \frac{d^2 u_1}{dz^2} + b_{22} \frac{d^2 u_2}{dz^2} - \frac{1}{2} d_{20} \frac{dv_0}{dz} - \frac{1}{2} d_{21} \frac{dv_1}{dz} - \frac{1}{2} d_{22} \frac{dv_2}{dz} - c_{12} u_1 - c_{11} u_2 &= 0 \\
e_{00} \frac{d^2 v_0}{dz^2} + e_{10} \frac{d^2 v_1}{dz^2} + e_{20} \frac{d^2 v_2}{dz^2} + \frac{1}{2} d_{10} \frac{du_1}{dz} + \frac{1}{2} d_{20} \frac{du_2}{dz} &= 0 \quad (\text{III-2}) \\
e_{10} \frac{d^2 v_0}{dz^2} + e_{11} \frac{d^2 v_1}{dz^2} + e_{12} \frac{d^2 v_2}{dz^2} + \frac{1}{2} d_{11} \frac{du_1}{dz} + \frac{1}{2} d_{21} \frac{du_2}{dz} - a_{11} v_1 - a_{12} v_2 &= 0 \\
e_{20} \frac{d^2 v_0}{dz^2} + e_{12} \frac{d^2 v_1}{dz^2} + e_{22} \frac{d^2 v_2}{dz^2} + \frac{1}{2} d_{22} \frac{du_2}{dz} - a_{12} v_1 - a_{22} v_2 &= 0
\end{aligned}$$

and the following boundary conditions at $z = \pm b$:

$$\begin{aligned}
\frac{du_1}{dz} &= 0, \quad \frac{du_2}{dz} = 0 \\
2e_{10} \frac{dv_0}{dz} + 2e_{11} \frac{dv_1}{dz} + 2e_{12} \frac{dv_2}{dz} + d_{11} u_1 + d_{21} u_2 &= -4P \\
2e_{20} \frac{dv_0}{dz} + 2e_{12} \frac{dv_1}{dz} + 2e_{22} \frac{dv_2}{dz} + d_{22} u_2 &= 0 \quad (\text{III-3})
\end{aligned}$$

where the coefficients b_{11} , etc. are defined in reference 1. To the above boundary conditions must be added the boundary condition of geometric constraint, namely

$$v_0(\pm b) = 0 \quad (\text{III-4})$$

The differential equations (III-2) are identical with those of reference 1 (eqs. (17) or (A12) therein) with u_0 set equal to zero. The characteristic equation is the same as in reference 1, that is the same as equation (I-2) of the present paper.

The solution of the differential equations (III-2), subject to the boundary conditions (III-3) and (III-4), leads to equations for the deformations $u_1(z)$, $u_2(z)$, ..., $v_2(z)$ as linear functions of P . The flexibility coefficient C_4 shown in figure 7(b) is obtained from the equation

$$C_4 P = v_1(b) \quad (\text{III-5})$$

after $v_1(b)$ is expressed in terms of P . The shear force F_2 in figure 7(b) is obtained as a linear function of P by integrating the shear flow in plate element 0-1 along a longitudinal section. The coefficient of P in the resulting expression represents the desired formula for the influence coefficient α_2 shown in figure 7(b).

REFERENCE

1. Lin, Chuan-jui; and Libove, Charles: Theoretical Study of Corrugated Plates: Shearing of a Trapezoidally Corrugated Plate with Trough Lines Permitted to Curve. Syracuse University Research Institute, Report No. MAE 1833-T2, June 1970 (NASA CR-1750).

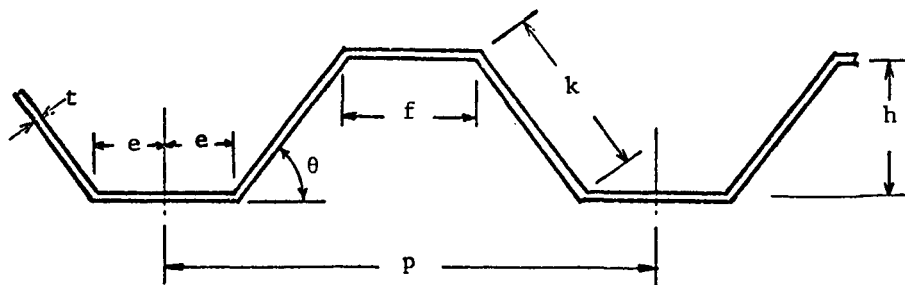
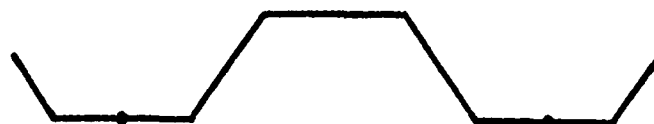


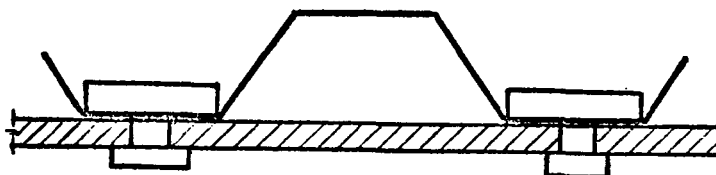
Figure 1. - Cross section considered.



(a) Point attachments at the ends of the trough lines.



(b) Point attachments at the ends of the trough lines and crest lines.



(c) Wide attachments to a rigid flange at the ends of the trough lines.

Figure 2. - Types of end attachments considered in reference 1.

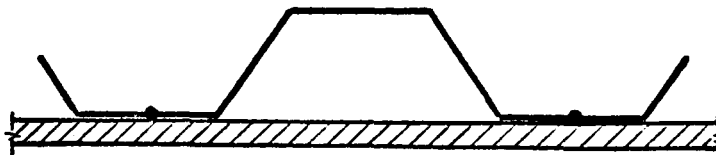


Figure 3. - Type of end attachments considered in the present paper.

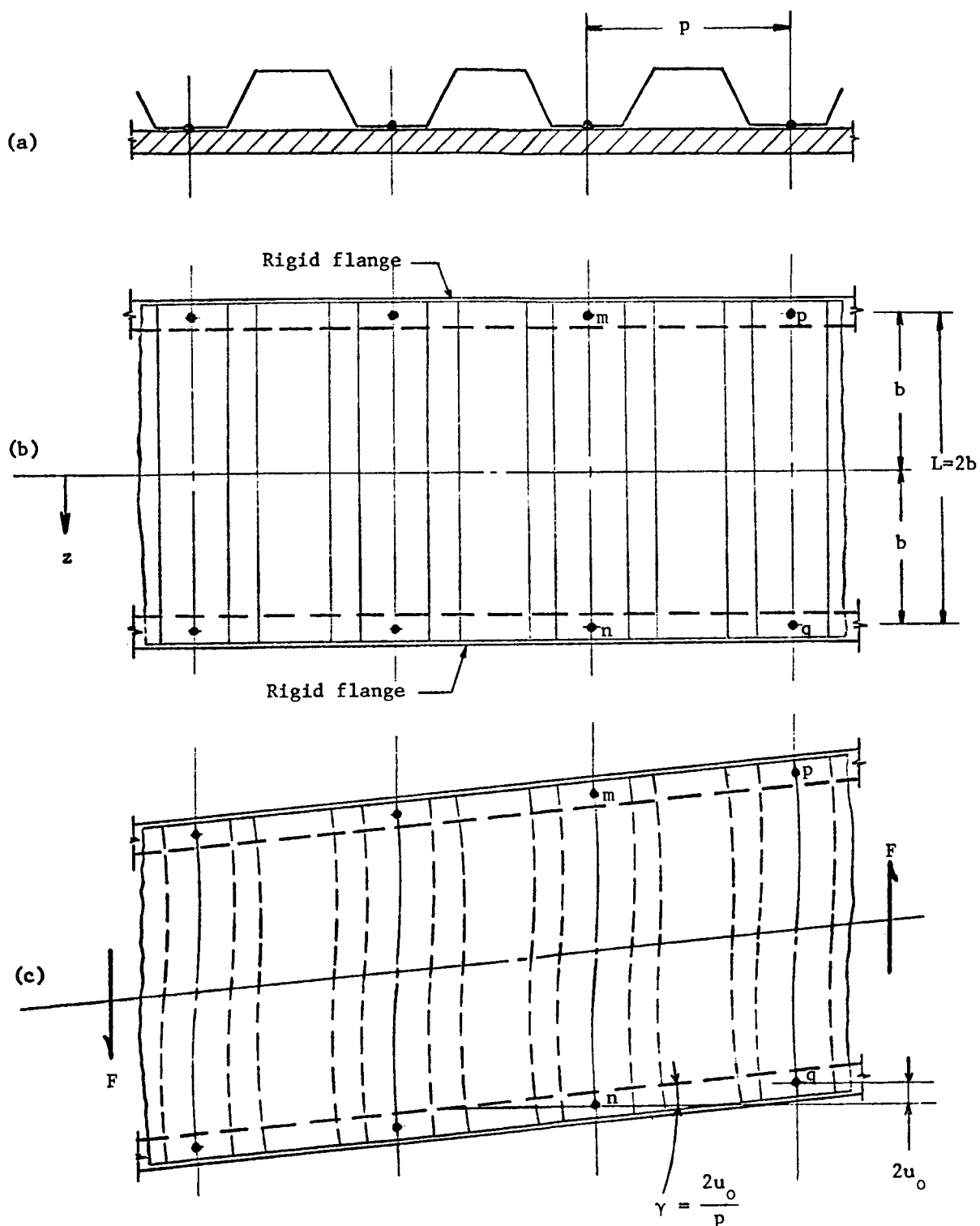


Figure 4. - (a) Front view and (b) top view of unsheared corrugated plate. (c) Top view of sheared corrugated plate.

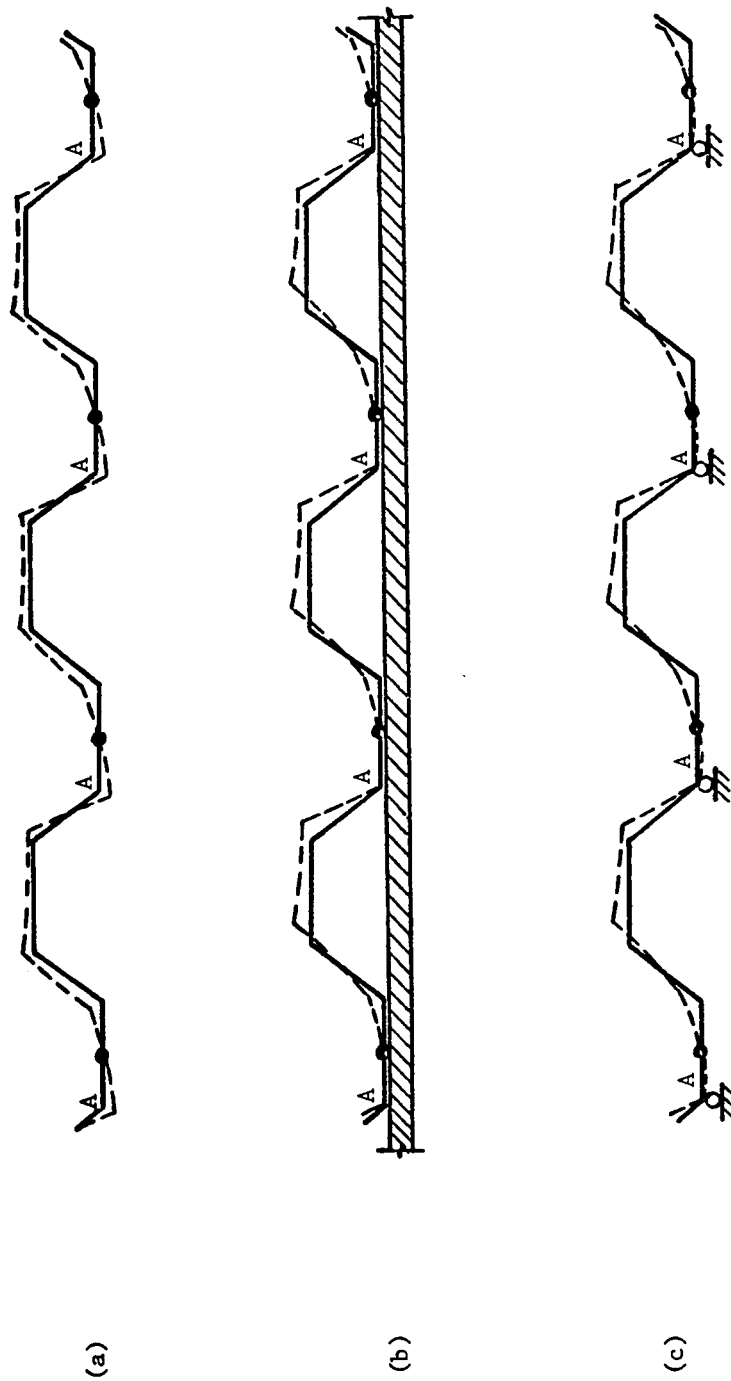
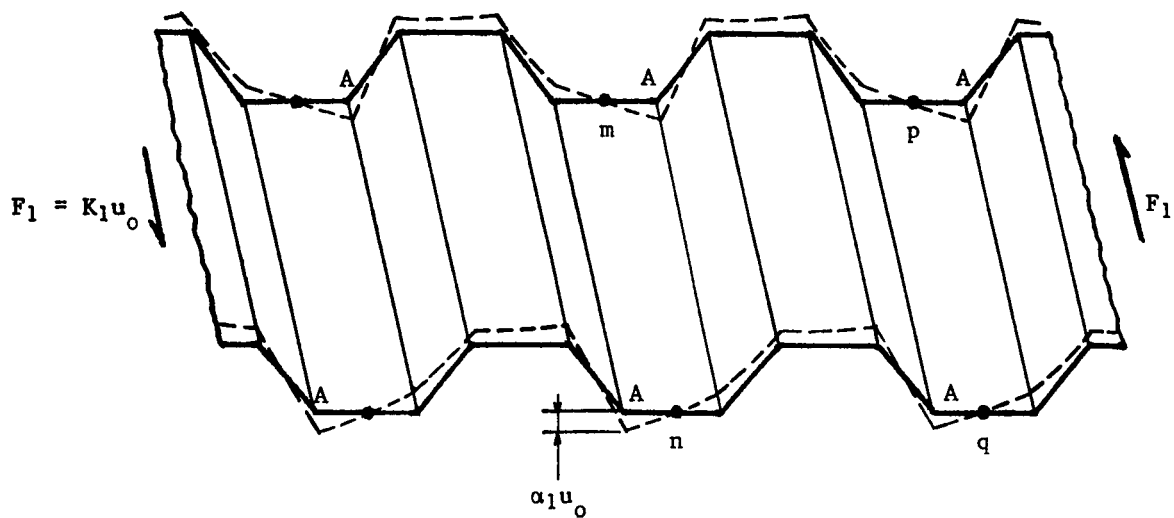
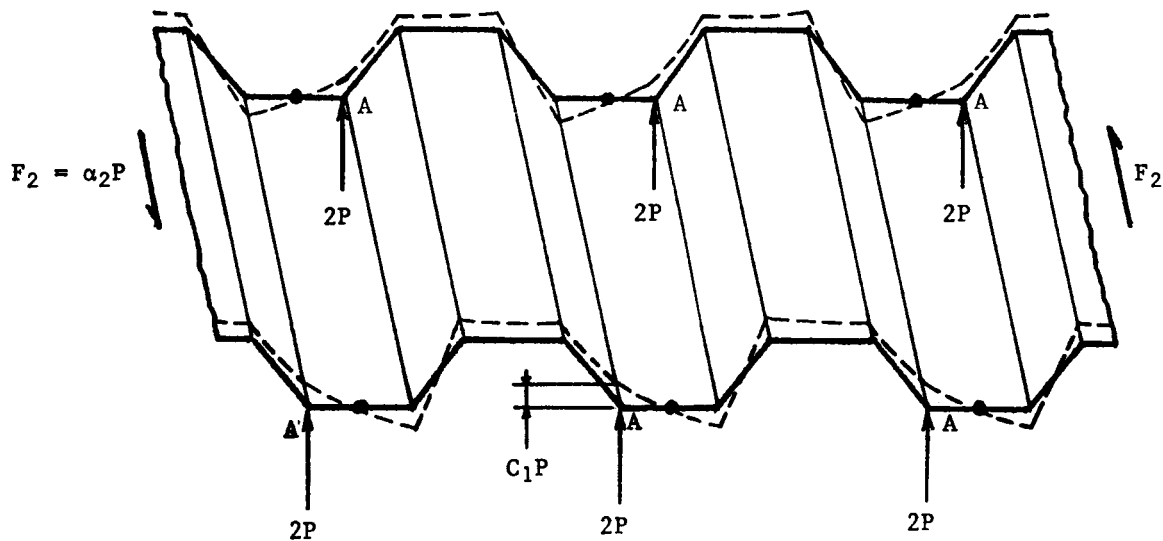


Figure 5. - (a) Deformation of end cross section ($z=b$) in the case of point attachments only. (b) Deformation of end cross section ($z=b$) in the case of point attachments to a rigid flange. (c) Simplified representation of rigid flange at $z=b$.

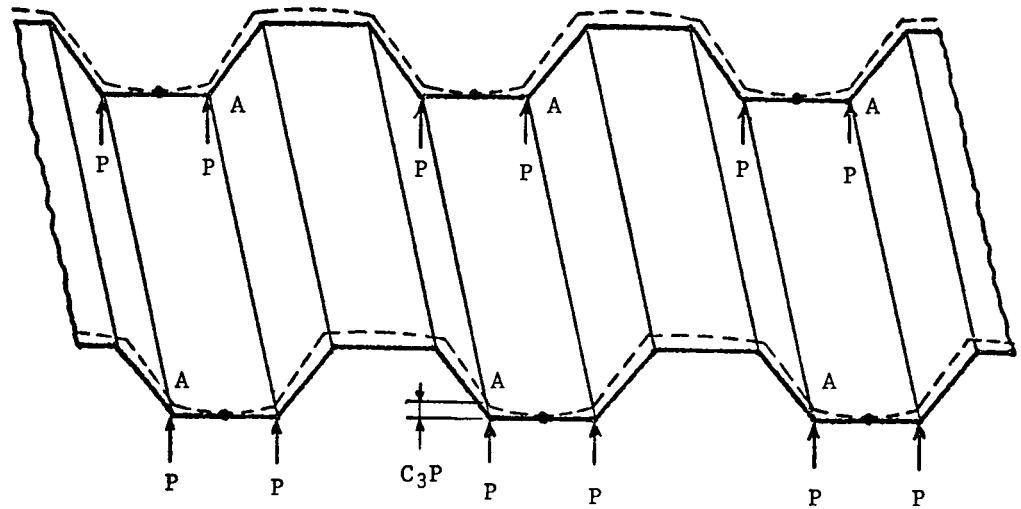


(a) Point attachments; overall shear deformation of $2u_0$ per corrugation.

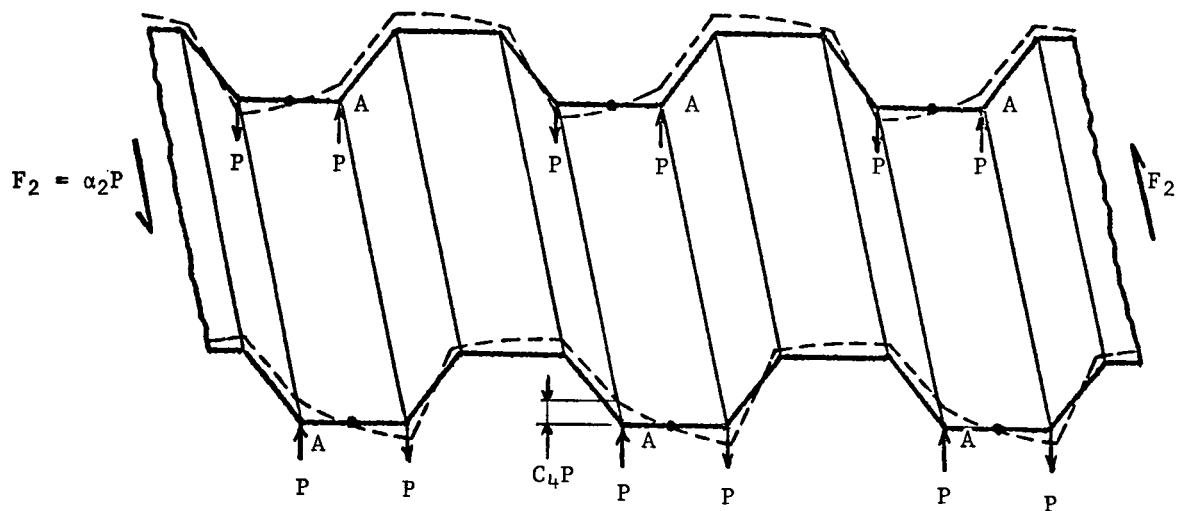


(b) Point attachments; zero overall shear deformation; concentrated upward loads of magnitude $2P$ at those corners which deflect downward in figure (a).

Figure 6. - Problems to be superimposed in order to represent the shearing of a corrugated plate with point attachments to a rigid flange.



(a) Symmetrical corner loads of magnitude P .



(b) Antisymmetrical corner loads of magnitude P .

Figure 7. - The loading of figure 6(b) decomposed into a symmetrical and an antisymmetrical component.

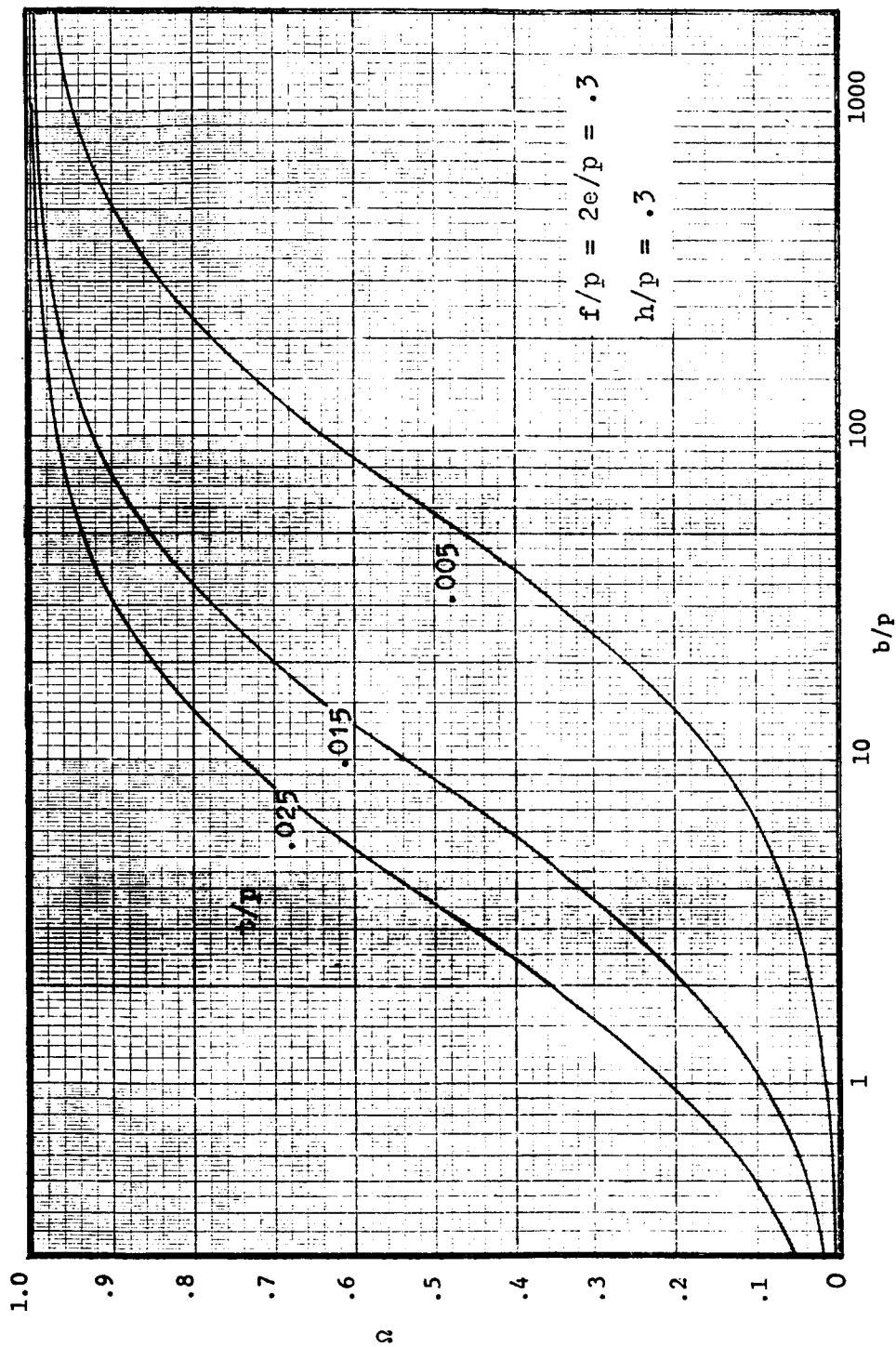


Figure 8. - Shear stiffness for a particular cross-sectional geometry ($f/p = .3$, $h/p = .3$) and three ratios of thickness to pitch.

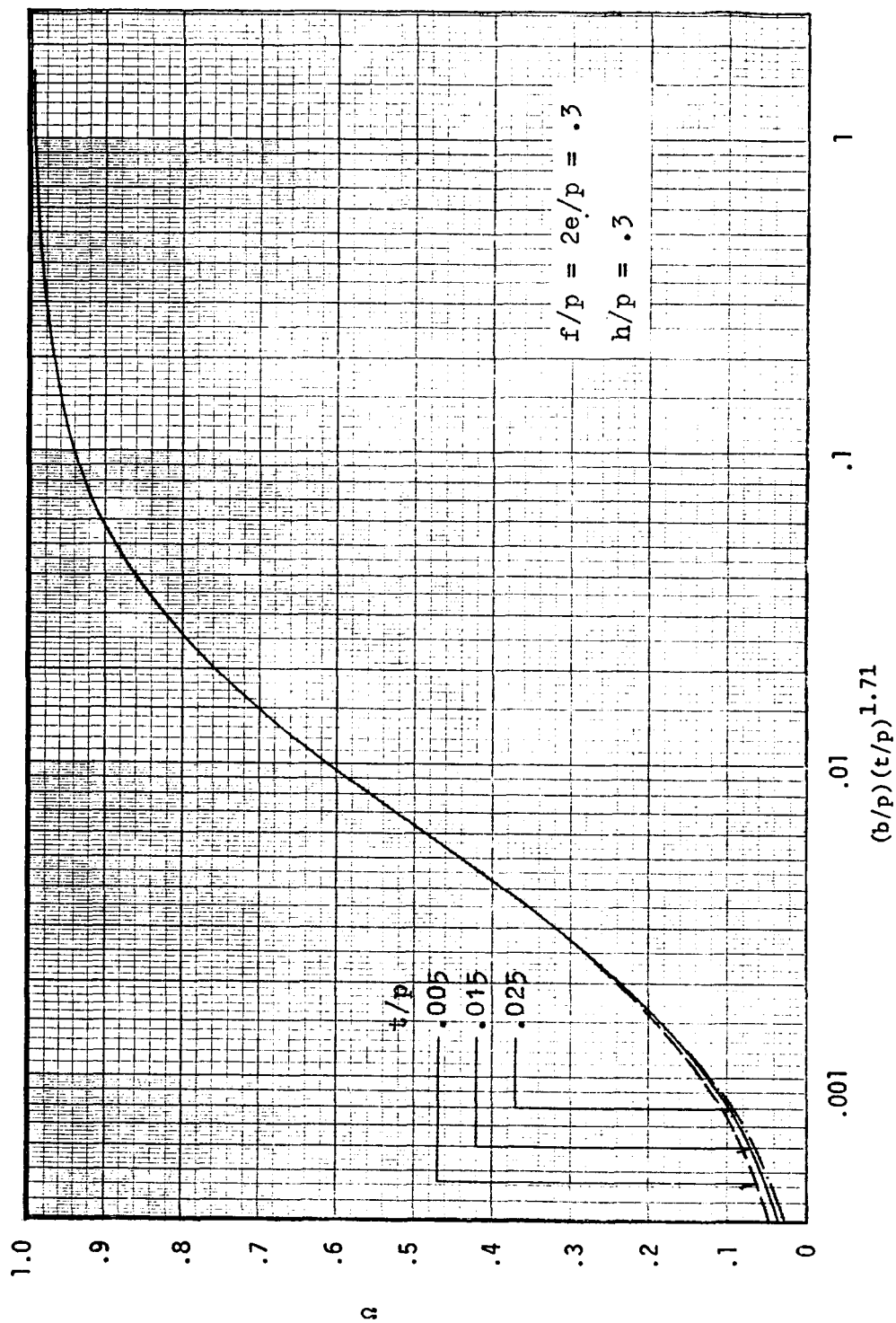


Figure 9. - Data of figure 8 replotted with t/p incorporated in the abscissa.

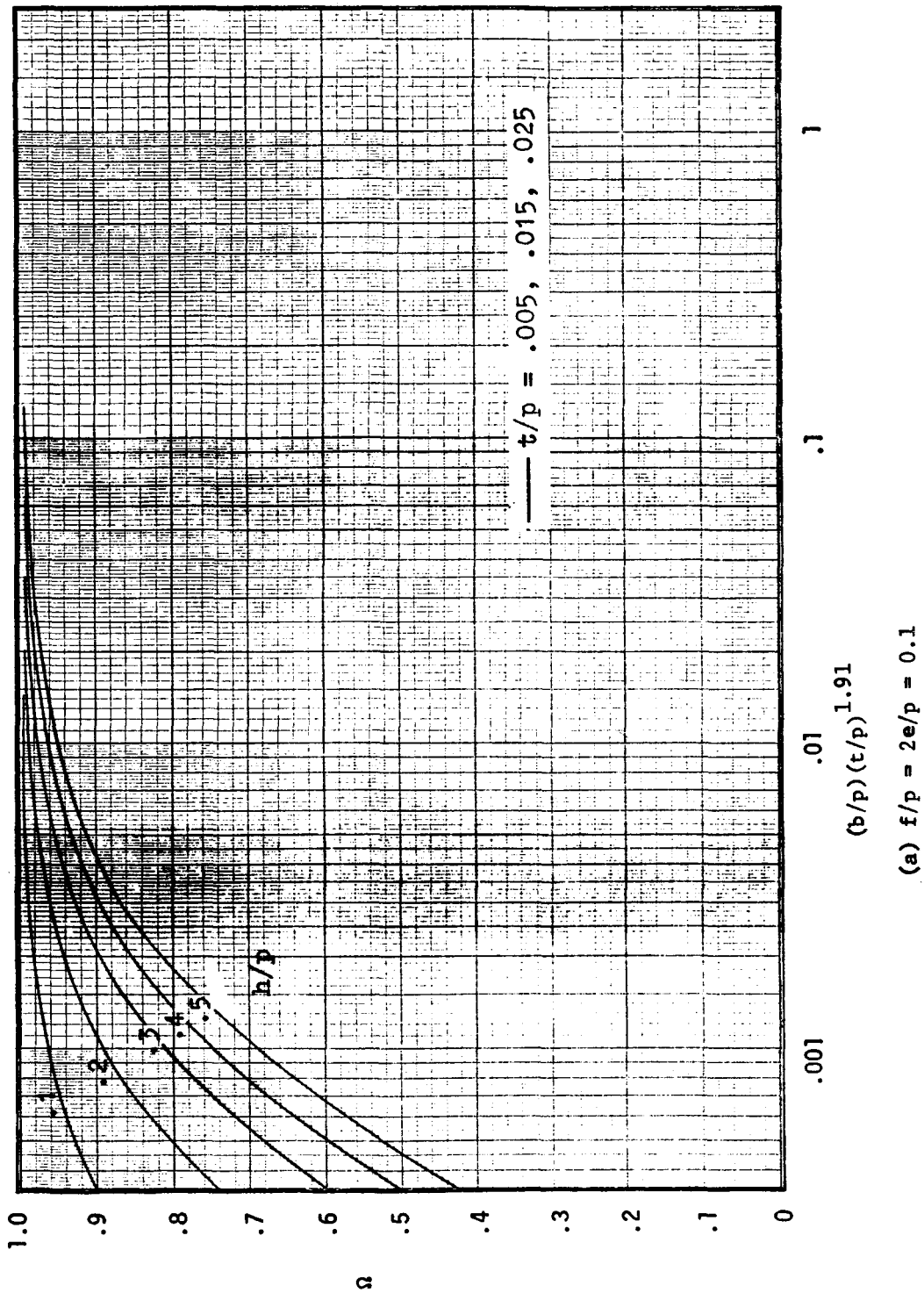
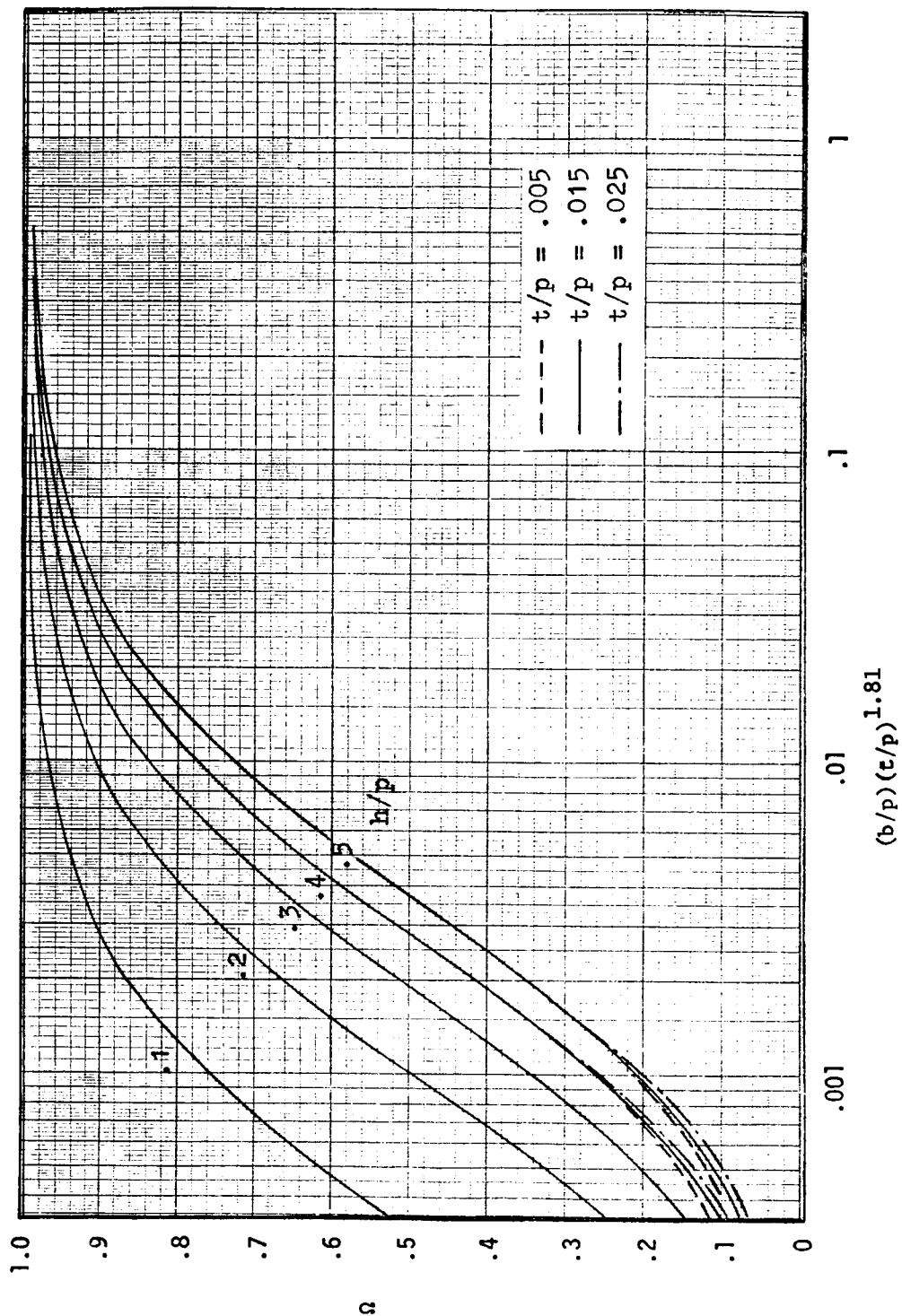
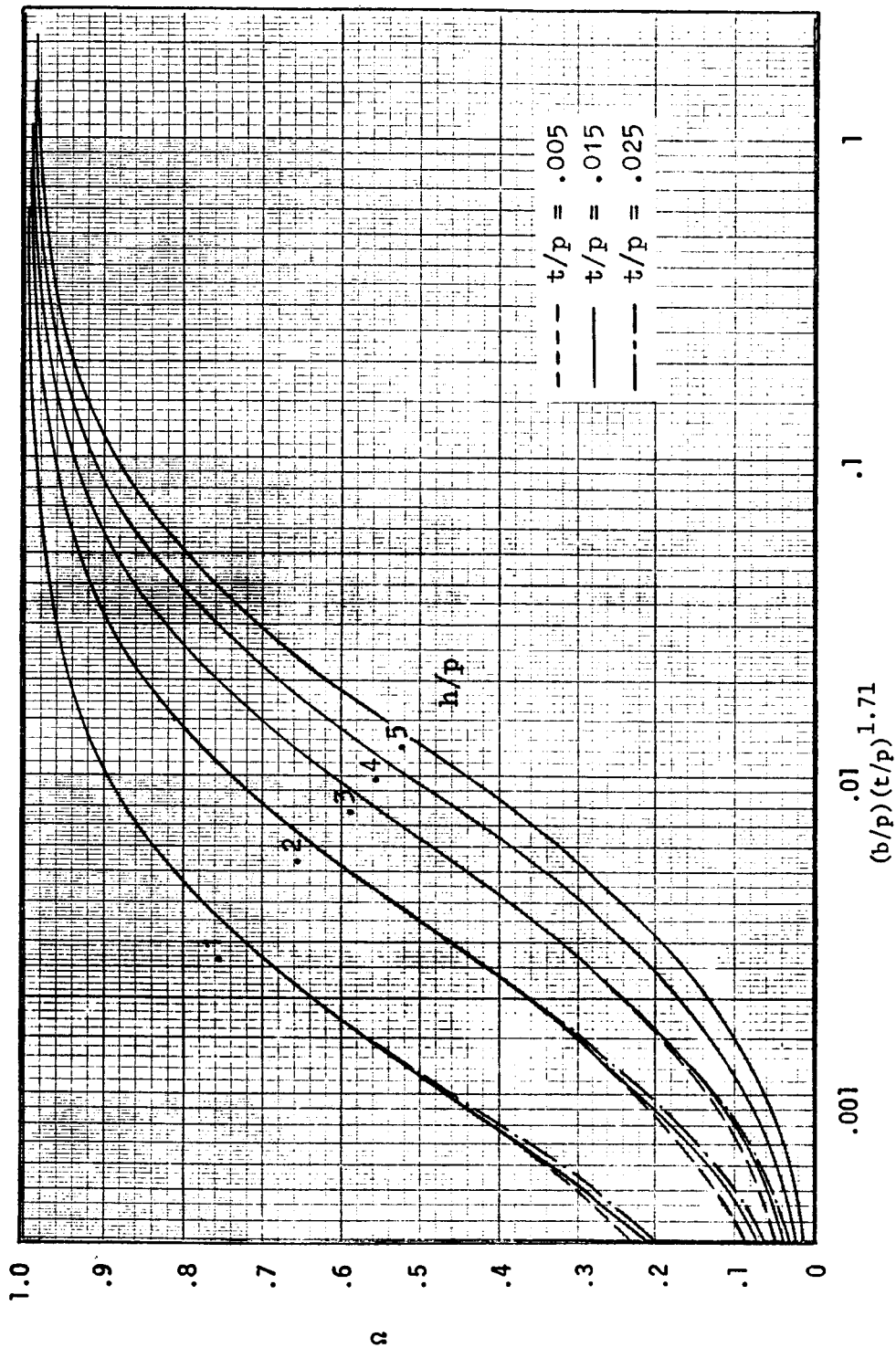


Figure 10. - Summary of all computed data on dimensionless stiffness Ω .



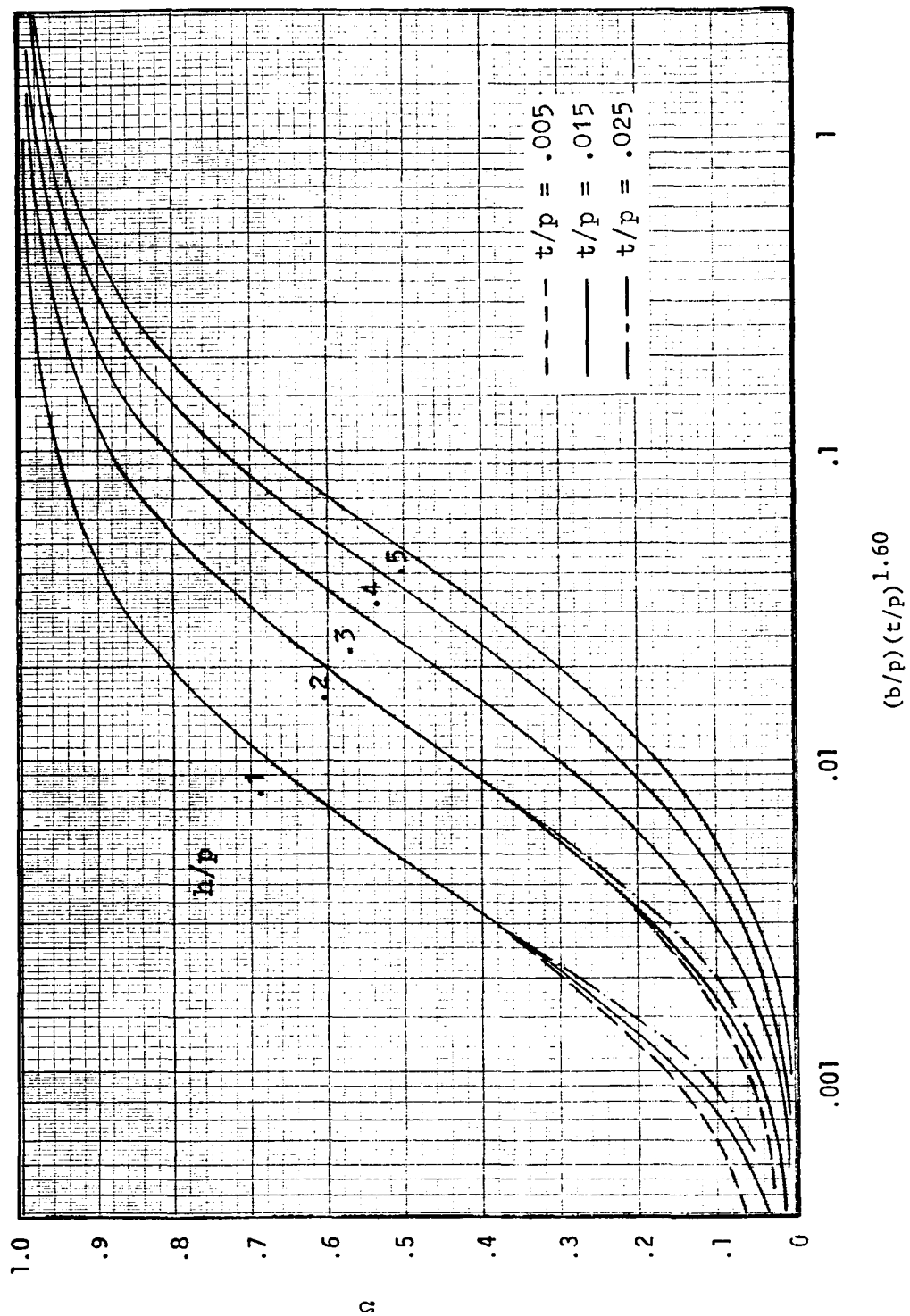
(b) $f/p = 2e/p = 0.2$

Figure 10. - Continued. (Where only one curve is shown, it applies to all three values of t/p .)



(c) $f/p = 2e/p = 0.3$

Figure 10. - Continued. (Where only one curve is shown, it applies to all three values of t/p .)



(d) $f/p = 2e/p = 0.5$

Figure 10. - Concluded. (Where only one curve is shown, it applies to all three values of t/p)

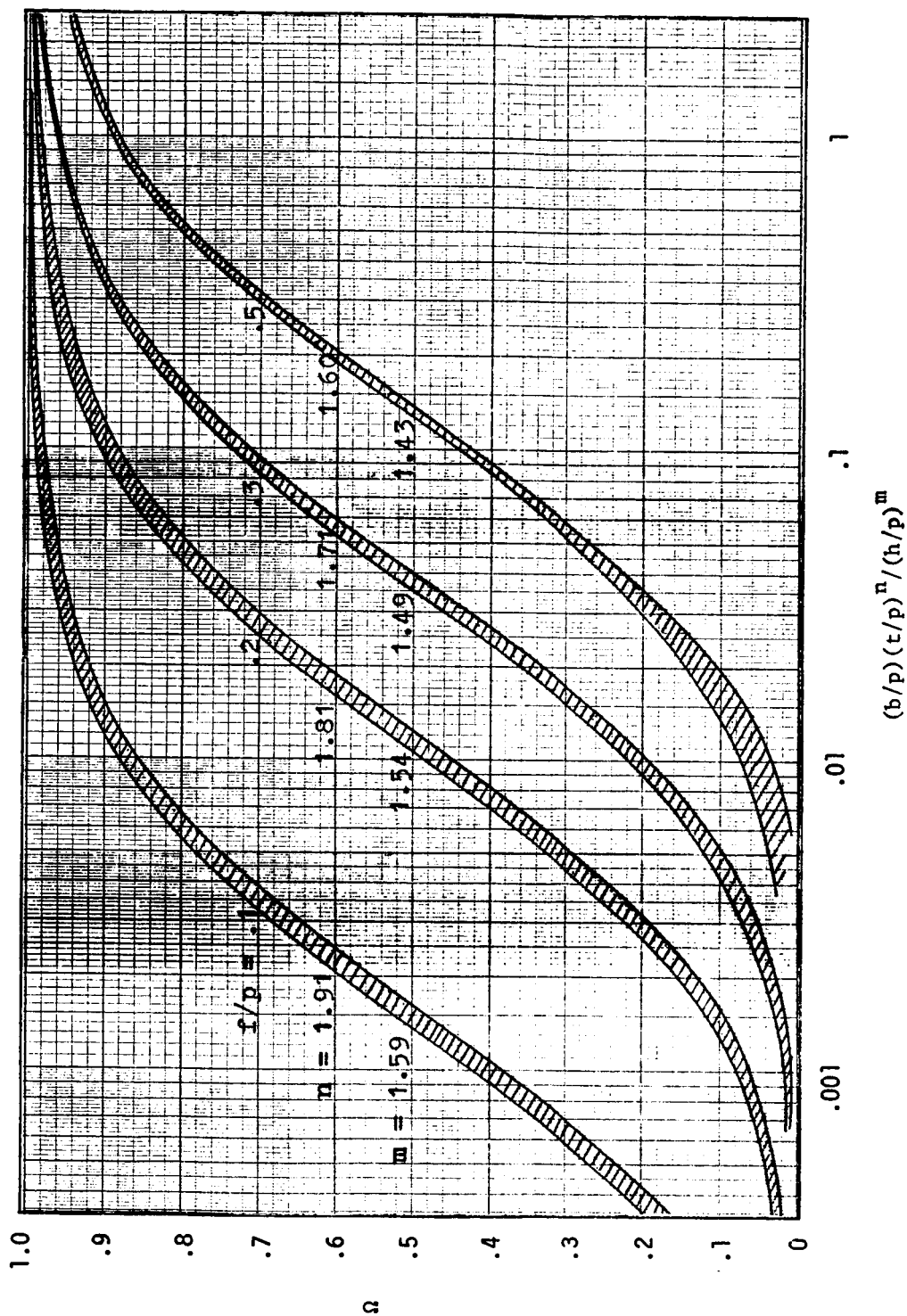


Figure 11. - Data of figure 10 replotted with h/p incorporated in the abscissa.

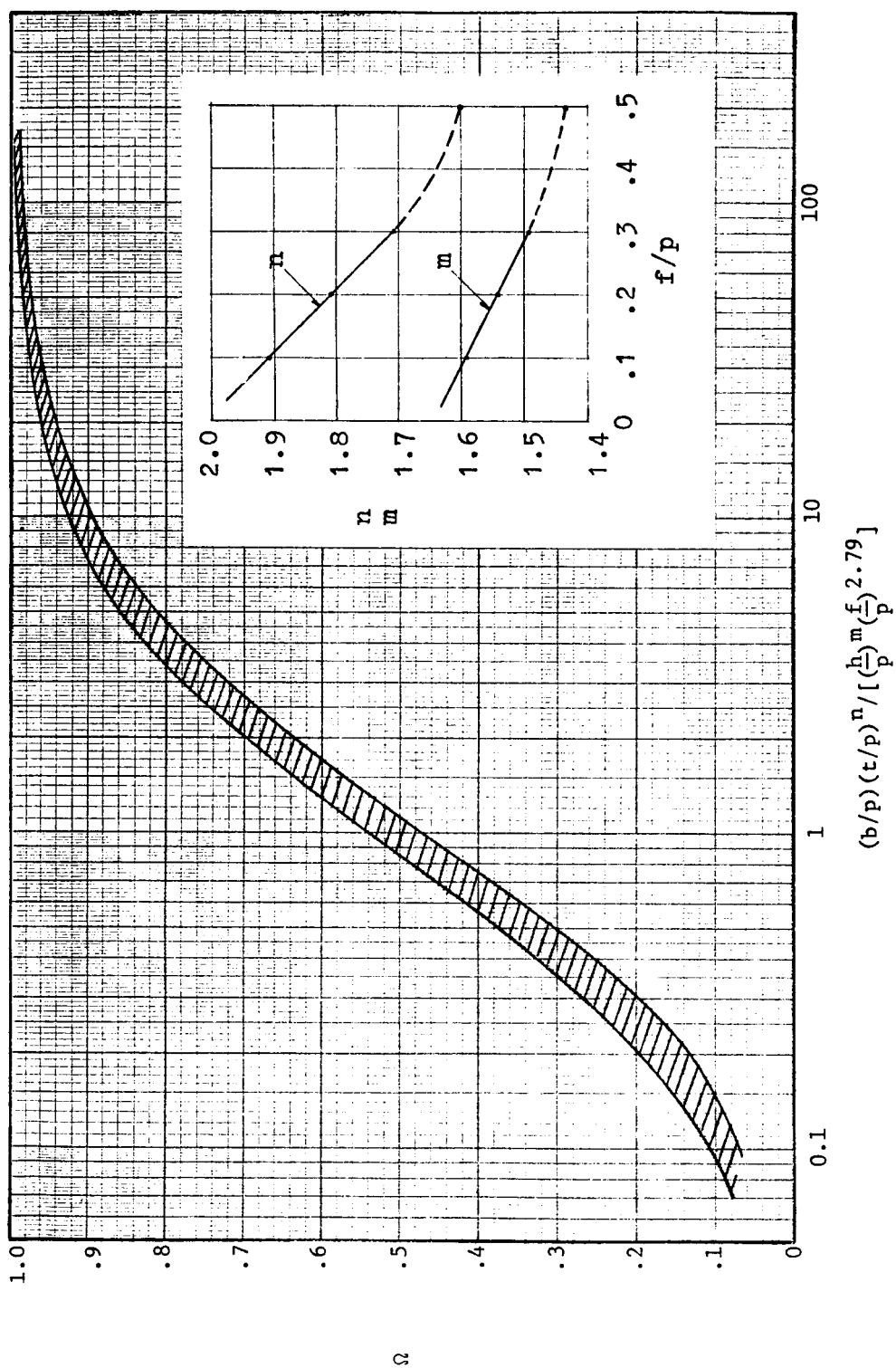


Figure 12. - Data of figure 11 replotted with f/p incorporated in the abscissa.

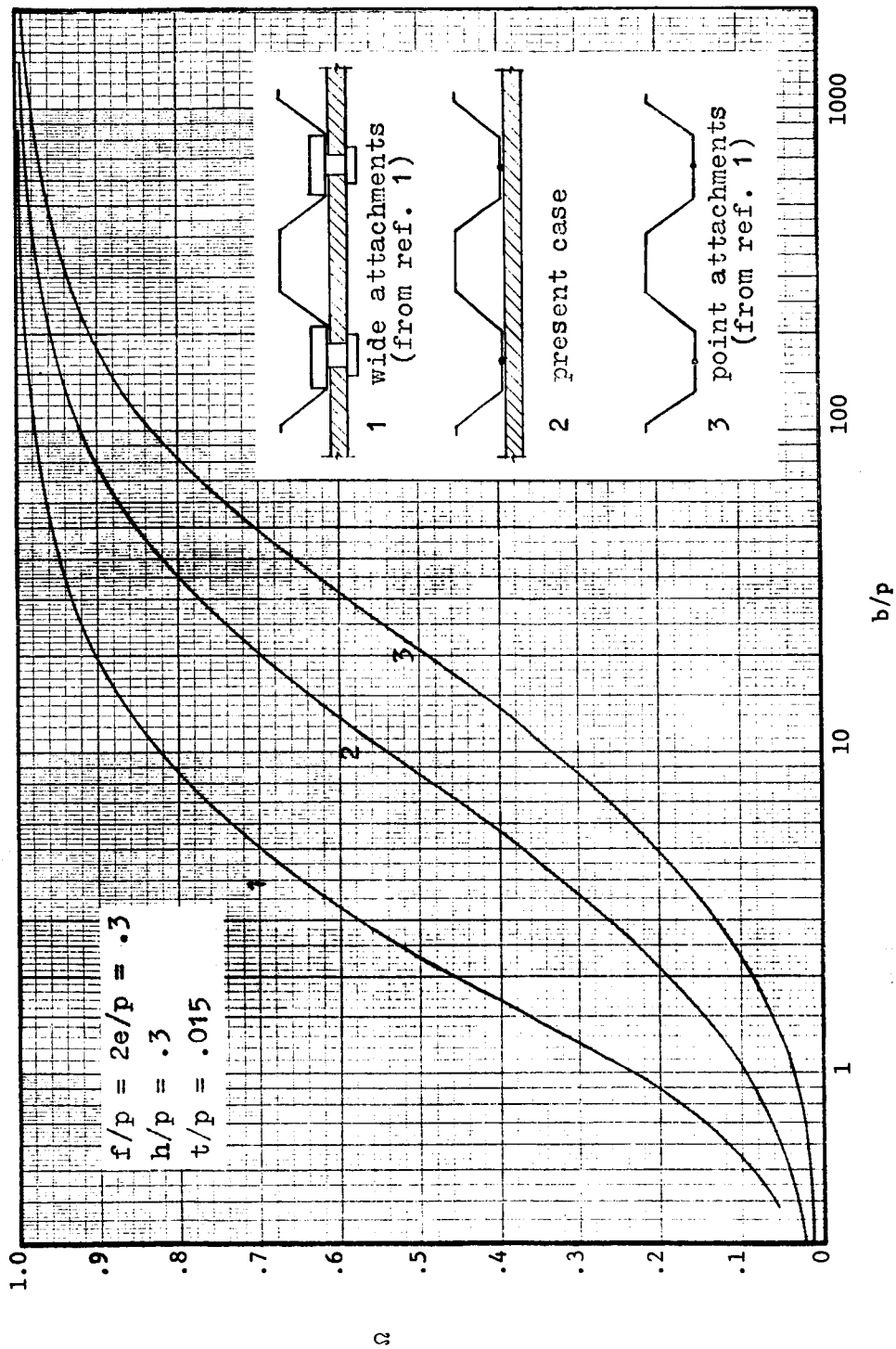


Figure 13. - Comparison of shear stiffness for three different end attachment conditions.

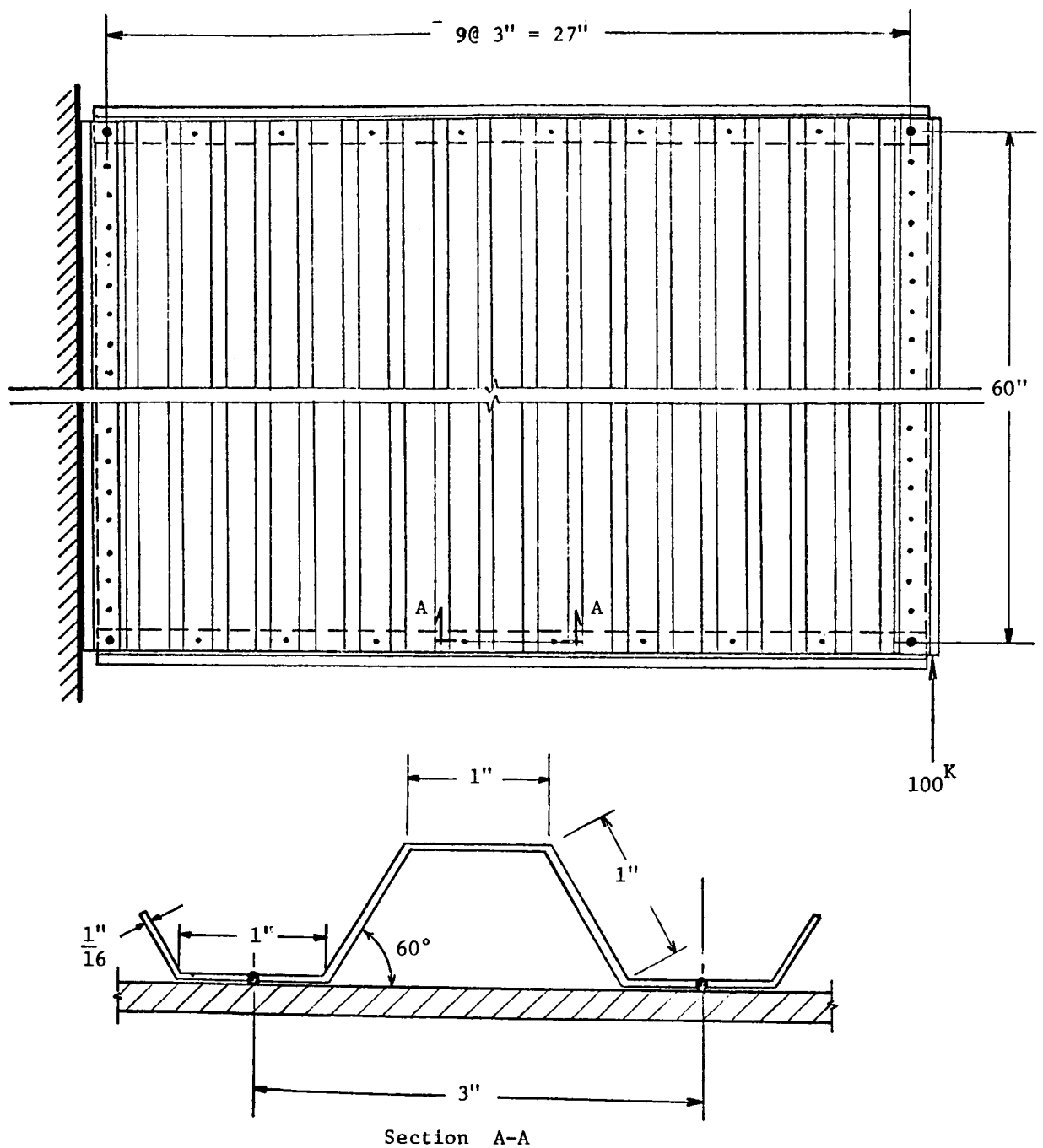
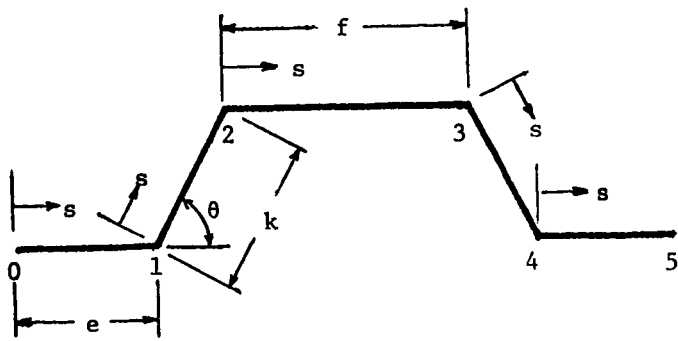
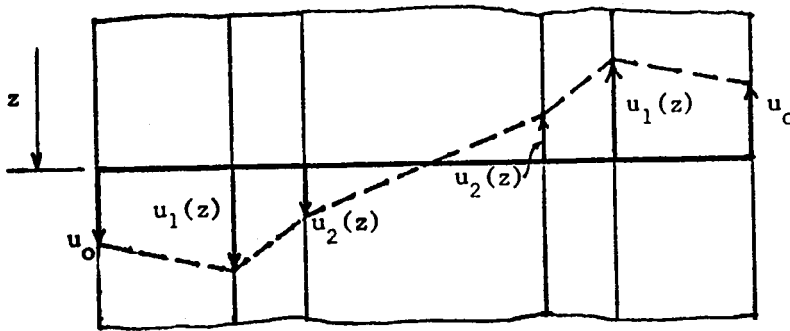


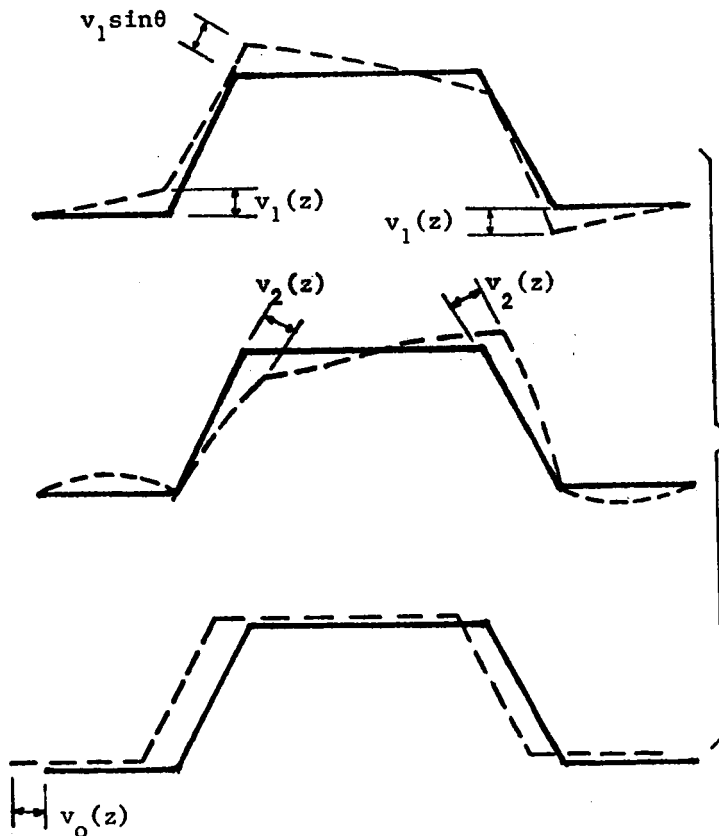
Figure 14. - Corrugated shear web in hinged picture frame test fixture, used for illustrative example.



(a) Typical cross section.

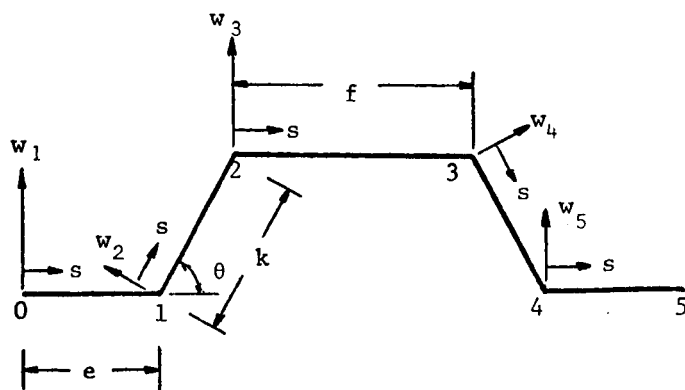


(b) Assumption regarding longitudinal displacements.

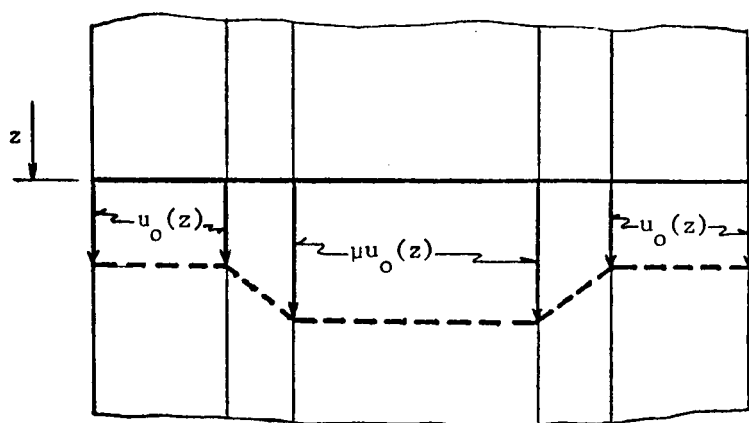


(c) Component modes for displacements in the plane of the cross section.

Figure 15. - Degrees of freedom of cross-sectional deformation assumed in the solution of problem I.

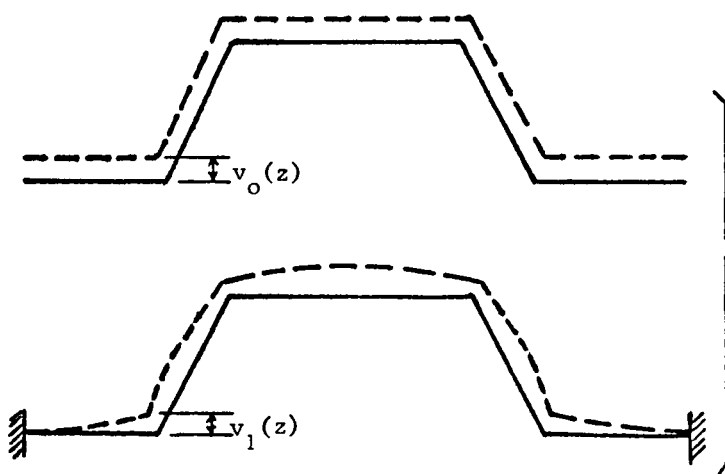


(a) Typical cross section.



(b) Assumption regarding longitudinal displacements.

$$(\mu \equiv -\frac{2e + k}{f + k})$$



(c) Component modes for displacements in the plane of the cross section.

Figure 16. - Degrees of freedom of cross-sectional deformation assumed in the solution of problem II.